

Supplementary Information

Designed Enhancement in Hydroxide Ion Conductivity of Viologen-Bakelite Organic Frameworks for Flexible Rechargeable Zinc-Air Battery

*Deepak Rase,^{a,b} Narugopal Manna,^{a,b} Rinku Kushwaha, Chitvan Jain, Himan Dev Singh,^{a,b} Pragalb Shekhar,^{a,b} Piyush Singh,^{a,b} Yashraj Kumar Singh^a and Ramanathan Vaidhyanathan^{*a,b,c}*

^aDepartment of Chemistry, Indian Institute of Science Education and Research, Dr. Homi Bhabha Road, Pashan, Pune 411008, India.

^bCentre for Energy Science, Indian Institute of Science Education and Research, Dr. Homi Bhabha Road, Pashan, Pune 411008, India.

^cThe Centre of Excellence for Carbon Capture & Removal, Svante Incorporation, 8800 Glenlyon Pkwy, Burnaby, British Columbia, V5J 5K3, Canada.

1. EXPERIMENTAL SECTION:

1. Materials and methods:

Paraformaldehyde and mesitylene were purchased from Spectrochem Pvt. Ltd. ; 1,2,4,5-Tetrakis(bromomethyl)benzene, 4-Pyridinecarboxaldehyde was purchased from TCI Chemicals (India) Pvt. Ltd. All other reagents were of analytical grade. All chemicals were used without any further purification.

2. Synthesis of polymer: The synthesis of two novel polymers, IISERP-POF12 (**2**) and IISERP-POF13 (**3**), from the monomers and its further conversion into **2_OH** and **3_OH** after the exchange of the Br- with OH- ions)

3. Physical Characterization:

Thermo-gravimetric analysis:

Thermo-gravimetric analysis was carried out on NETSZCH TGA-DSC system. The TGAs were performed under N₂ gas flow (20 mL/min) (purge + protective) and samples were heated from room temperature to 550 °C at a ramp rate of 5 °C/min.

¹³C Solid-State Nuclear Magnetic Resonance (NMR) Spectroscopy:

High-resolution solid-state NMR spectrum was recorded at ambient pressure on a Bruker AVANCE III spectrometer using a standard CP-TOSS pulse sequence (cross polarization with total suppression of sidebands) probe with 4 mm (outside diameter) zirconia rotors.

Infra-Red Spectroscopy:

IR spectra were obtained using a Nicolet ID5 attenuated total reflectance IR spectrometer operating at ambient temperature. The solid-state IR spectra were recorded using KBr pellets as background.

Field Emission-Scanning Electron Microscopy (FESEM):

Electron Microscope with integral charge compensator and embedded EsB and AsB detectors. Oxford Xmax instruments 80 mm². (Carl Zeiss NTS, GmbH), Imaging conditions: 2kV, WD= 2 mm, 200 kX, Inlens detector. For SEM images, as an initial preparation, the samples were ground thoroughly, soaked in ethanol for 30 min. and were sonicated for 2 h. These well dispersed samples were drop-casted on the silicon wafer and dried under vacuum for 12 h.

High resolution Transmission Electron Microscopy (HR-TEM):

Transmission electron microscopy (TEM) was performed using a JEM 2200FS TEM microscope operating at an accelerating voltage of 200 kV). The diffractograms were recorded at a scanning rate of 1° min⁻¹ between 20° and 80°.

Adsorption study

Adsorption studies were carried out using a Micromeritics 3-FLEX pore and surface area analyser.

4. Solid-state ZAB demonstration:

Preparation of the Gel Electrolytes:

To prepare the mixture, 100 mg of 3_OH powder was dispersed in 2 ml of water and stirred at 90°C for 1 hour until a uniform distribution of the polymer was achieved. Subsequently, 100 mg of PVA was introduced into the same solution, and the mixture was heated for 3 hours to ensure a homogeneous blend of POF (3_OH) and PVA. As soon as the PVA had completely dissolved in the water, the solution was poured into a petri dish and promptly subjected to a cooling process. The cooling procedure involved two stages: initially at -20 °C for 3 hours, followed by a subsequent stage at 0 °C for 2 hours. After this cooling process, the resultant membrane solidified. The solidified membrane was then air-dried at room temperature, resulting in the formation of a flexible membrane. This flexible membrane was subsequently employed as a combined separator and electrolyte within the context of a Zinc air battery application.

Assembly and test of solid-state ZAB device:

The construction of the solid-state rechargeable zinc-air battery (ZAB) involved the following components: zinc powder as the anode, a gas diffusion layer (GDL) coated with Pt/C +RuO₂ as the air-cathode, and a PVA/KOH gel serving as the electrolyte. This assembly was set up within an electrochemical ZAB device arrangement provided by MTI Corporation. To prepare the catalyst slurry, Pt/C +RuO₂ was mixed with a 1:4 ratio mixture of isopropyl alcohol and water, followed by an hour of sonication. Subsequently, 10 wt% Fumion solution was added to the resulting dispersion, and the mixture underwent an additional hour of sonication. Once the dispersion was fully achieved, the catalyst slurry was applied to a gas diffusion layer (GDL) and allowed to dry at 60°C for 12 hours, resulting in a catalyst loading of 1.0 mg cm⁻² (with an electrode area of 1.0 cm²). For the evaluation of the ZAB setup using a multichannel CH instrument was employed under room temperature conditions. The analysis of the ZAB involved steady-state polarization conducted at a scan rate of 10 mV s⁻¹. Additionally, polarization analysis and electrochemical impedance spectroscopy (EIS) studies were performed at a constant voltage of 1.0 V with a 20 mV amplitude. Galvanostatic discharge and discharge-charge cycling tests (consisting of 15 minutes of discharge followed by 15 minutes of charge) were carried out using a CH- potentiostat.

Fabrication of flexible solid-state ZAB:

For the flexible solid-state Zinc-air battery, Zn foil with 0.10 mm thickness was employed as the anode, Pt/C + RuO₂ coated carbon cloth was used as the air-breathing cathode and hydroxide ion conducting 3_OH@PVA as the solid-state separator-cum-electrolyte. During the fabrication of the battery, 3_OH@PVA was wetted with 300 µL 3 M KOH solution. The anode and cathode were separated with 3_OH@PVA and the sandwich is sealed. The backside of the cathode was kept it open for the passage of air and the battery was operated without providing any additional O₂ supply.

Electrochemical Measurements:

The linear sweep voltammetry and the constant current charge-discharge measurements were performed using the AMETEK Battery analyser using VERSA STUDIO (Version 2.52) software.

Impedance measurements:

The Solartron SI 1260 IMPEDANCE/GAIN-PHASE ANALYZER model was used to carry out the impedance measurement. The impedance spectra were recorded by applying a range of frequencies from 1 MHz to 0.1 Hz with an amplitude of 10 mV. Moreover, ESPEC SH-222 Bench-top Type Temperature & Humidity Chamber was used to maintain the temperature and humidity while measurement. Impedance data fitting was done using Z-view software.

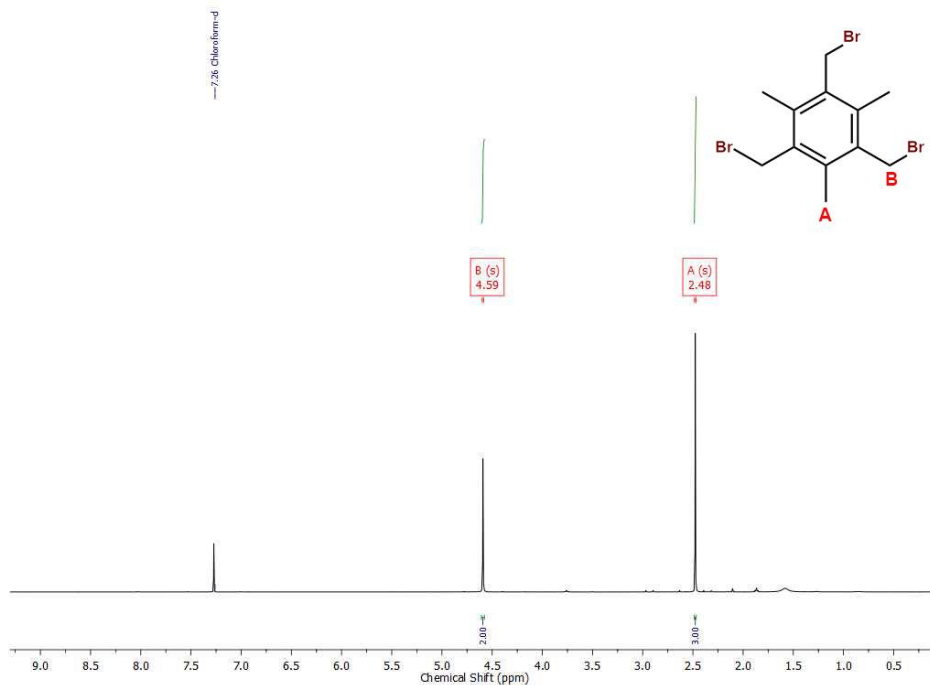
Experimental conditions of hydroxyl ion conductivity in pellet form	Temperature range for impedance measurements	30 °C to 80 °C
	Relative humidity for impedance measurements	30% to 95 %
	Frequency range for impedance measurements	10 ⁶ Hz to 0.1 Hz
	AC amplitude for impedance measurements	10 mV
Experimental conditions of electronic conductivity in pellet form	Electronic conductivity of 2_OH and 3_OH computed from linear sweep voltammetry (LSV) with the scan rate	10 mV s ⁻¹
	Potential window used for linear sweep voltammetry (LSV)	-1 to 1 V
Experimental conditions rechargeable Zinc-air battery	Frequency range for impedance measurements in ZAB cell	10 ⁶ Hz to 0.1 Hz
	Current density for discharge process was at voltage of 1.38 V	10 mA cm ⁻²
	Steady-state polarization of ZAB cell conducted at a scan rate	10 mV s ⁻¹

2.Synthesis of Polymers

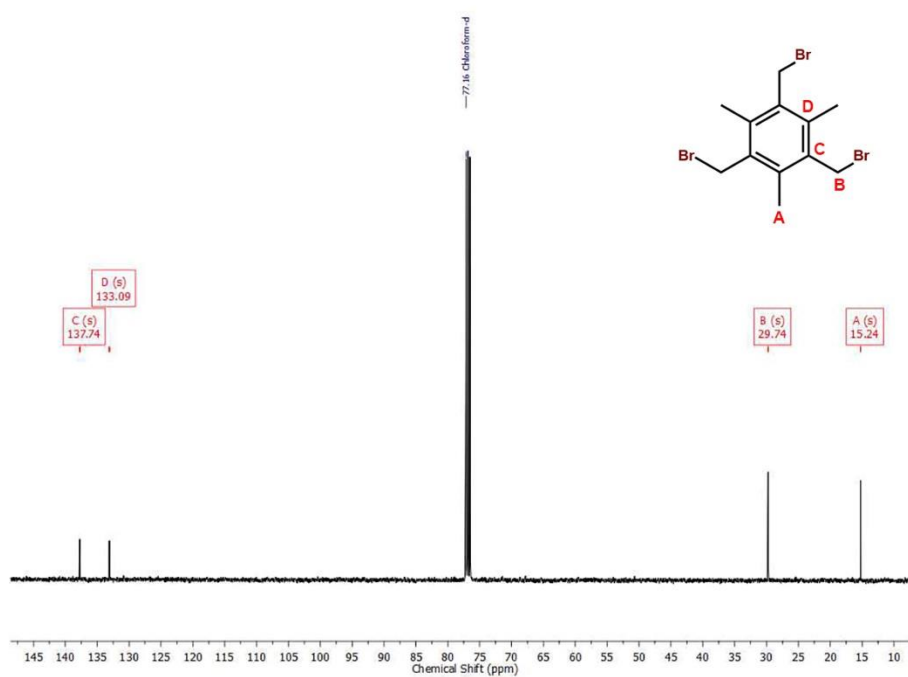
2.1 Synthesis of 1,3,5-tris(bromomethyl)-2,4,6-trimethylbenzene

To a mixture of mesitylene (6.0 g, 50 mmol), paraformaldehyde (6.0 g, 200 mmol) and 30 mL of glacial acetic acid was added 40 mL of 33% HBr in acetic acid. The reaction mixture was kept at

110 °C for 12 hours. After cooling down to room temperature, the reaction mixture was poured into ice water. The products precipitated out, were filtered off, washed several times with distilled water to make it acid free. The compound was dried over P2O5 giving dirty yellow solid. Yield ~ 92%; ^1H NMR (400 MHz, CDCl_3) δ 4.59 (s, 1H), 2.48 (s, 1H). ^{13}C NMR (101 MHz, CDCl_3) δ 137.74 (s), 133.09 (s), 29.74 (s), 15.24 (s).



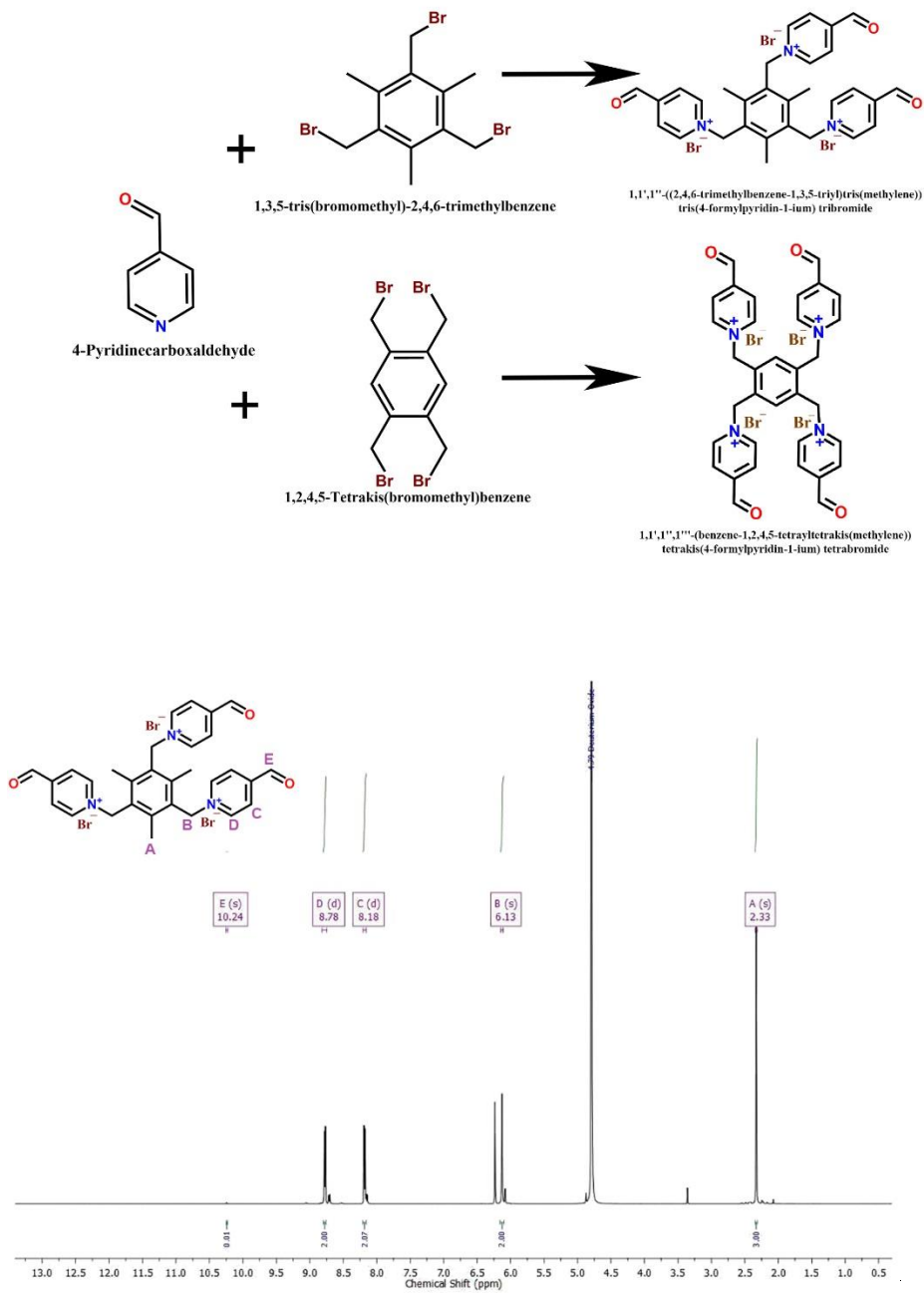
^1H NMR of 1,3,5-tris(bromomethyl)-2,4,6-trimethylbenzene



^{13}C NMR of 1,3,5-tris(bromomethyl)-2,4,6-trimethylbenzene

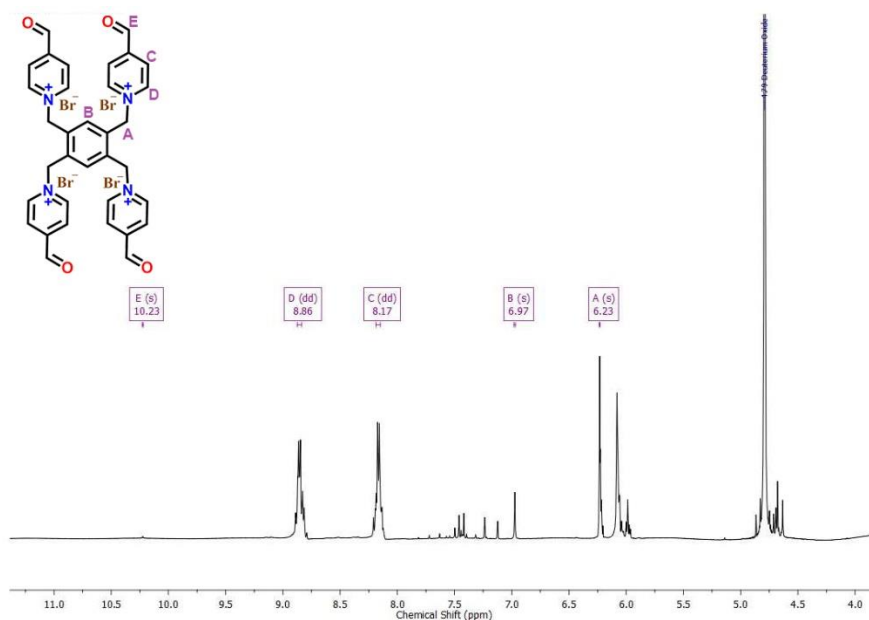
2.2 Synthesis of Aldehyde Monomers

Typically, **1,3,5-tris(bromomethyl)-2,4,6-trimethylbenzene** (398 mg, 1 mmol) or 1,2,4,5-Tetrakis(bromomethyl)benzene (450 mg, 1 mmol) and 4-Pyridinecarboxaldehyde (642-856 mg, 6-8 mmol) were added in acetonitrile (40 mL) and the reaction mixture was refluxed overnight at 85 °C. The resulting precipitate was filtered off and washed with acetone. to give the pure products.



^1H NMR of 1,1',1''-((2,4,6-trimethylbenzene-1,3,5-triyl)tris(methylene))tris(4-formylpyridin-1-ium) tribromide

^1H NMR (400 MHz, D₂O) δ 10.24 (s, 1H), 8.78 (d, J = 6.8 Hz, 1H), 8.18 (d, J = 6.6 Hz, 1H), 6.13 (s, 1H), 2.33 (s, 1H).

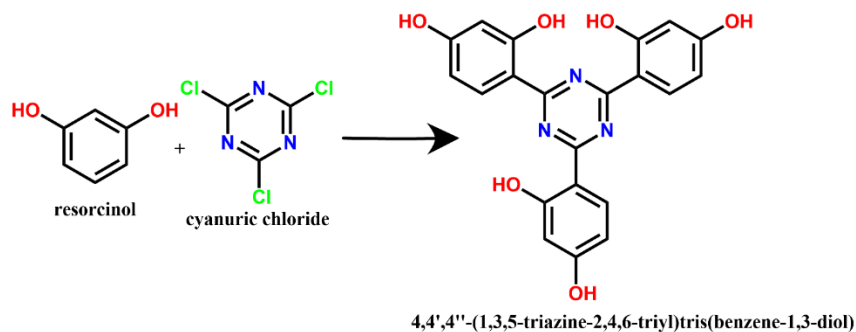


^1H NMR of 1,1',1'',1'''-(benzene-1,2,4,5-tetrayltetrakis(methylene))tetrakis(4-formylpyridin-1-ium) tetrabromide

^1H NMR (400 MHz, D₂O) δ 10.23 (s, 1H), 8.86 (dd, J = 6.4, 3.4 Hz, 3H), 8.17 (dd, J = 10.3, 4.0 Hz, 3H), 6.97 (s, 1H), 6.23 (s, 1H).

2.3 Synthesis of 4,4',4''-(1,3,5-triazine-2,4,6-triyl)tris(benzene-1,3-diol) (TRIRES)

The synthesis of the compound is based on a previous report.^[S2] 2 g (10.8 mmol) of cyanuric chloride and 3.58 g (32.5 mmol) of resorcinol were dispersed in 100 mL of 1,2-dichloroethane. Contents were dissolved by heating at 75 °C, following this, the mixture was cooled to 0 °C. To this, about 4.35 g (32.5 mmol) anhydrous AlCl₃ was slowly added in 30 minutes. This mixture was refluxed for 36 h. The reaction mixture was cooled to room temperature and the solvent was removed using a rota-evaporator. The solid was then stirred in 100 mL of 10% HCl for 3 h and kept it for an additional 3 h. A yellow solid was precipitated, which was filtered under vacuum and washed with about 250 mL of diethyl ether to remove any unreacted starting materials. The product was dried in a vacuum oven. About 3.2 g (yield: 88%) of the product was obtained.

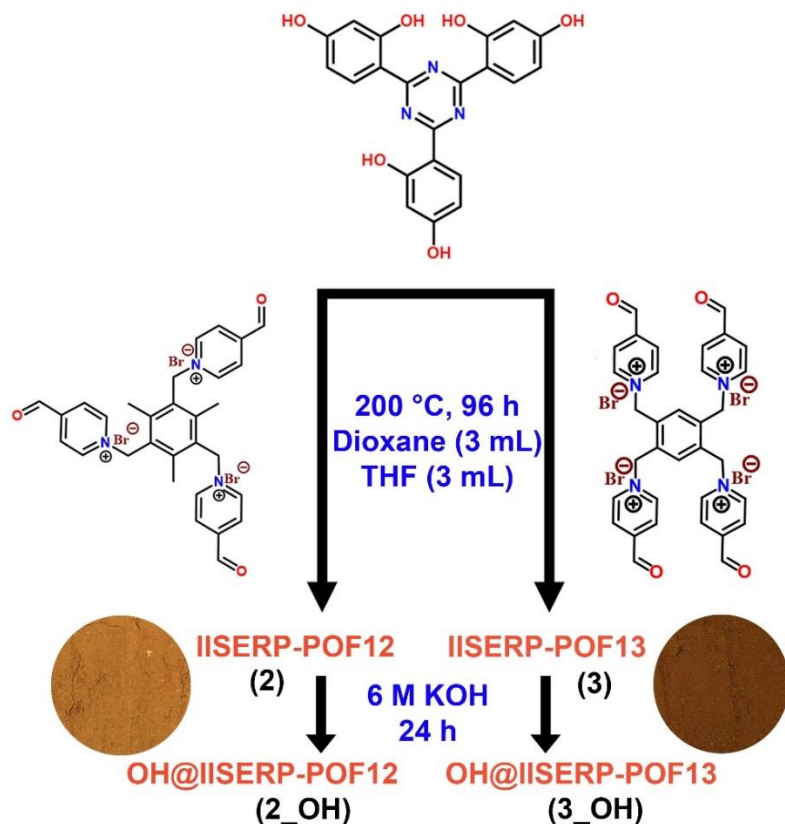


2.4 Synthesis of cationic polymer IISERP-POF12 (**2**) and IISERP-POF13 (**3**)

The polymer has been synthesized according to the optimized protocol by our group.^[S3] The solvothermal reaction between 0.2 mmol phenolic compound and 0.2 (for **2**)-1.5 (for **3**) mmol viologen aldehyde in a mixture of 3 mL THF and 3 mL 1,4- dioxane at 200 °C for 72 h yielded a brown-colored precipitate which was sequentially washed with DMF, THF, MeOH and finally acetone. The product was dried in the vacuum oven for 6 h and the obtained material was named hereafter as **2** and **3**. A significant colour difference was observed in compound **2** and **3**.

2.5 Anion exchange with IISERP-POF12 (**2**) and IISERP-POF13 (**3**) to form IISERP-POF12_OH (**2_OH**) and IISERP-POF13_OH (**3_OH**)

The as-made polymer **2** or **3** (100 mg) was dispersed in 10 mL of 6 M KOH and sonicated for 10 minutes. After sonication, the mixture was stirred for 24 h at room temperature for hydroxide ion (OH⁻) incorporation. Hydroxide ion exchanged polymer was filtered and washed with an ample amount of water to remove the excess KOH. The product was dried in a vacuum oven for 12 h at 80 °C and obtained a yield of 89 %.



Scheme1: Schematic showing the synthesis of 2, 3, 2_OH and 3_OH . Inset showing the photographic image of the compound.

3. Physical Characterization:

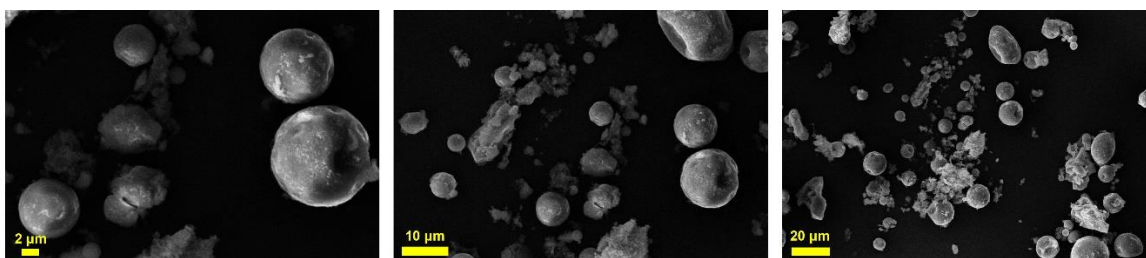


Fig. S1: Field Emission-Scanning Electron Microscopy (FESEM) images of 2 at different magnifications.

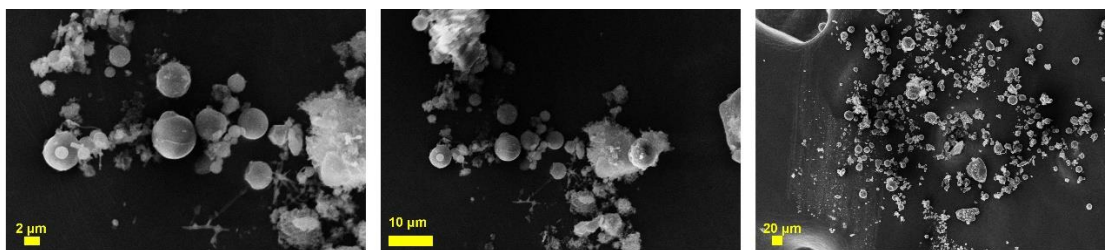


Fig. S2: FESEM images of **2_OH** at different magnifications.

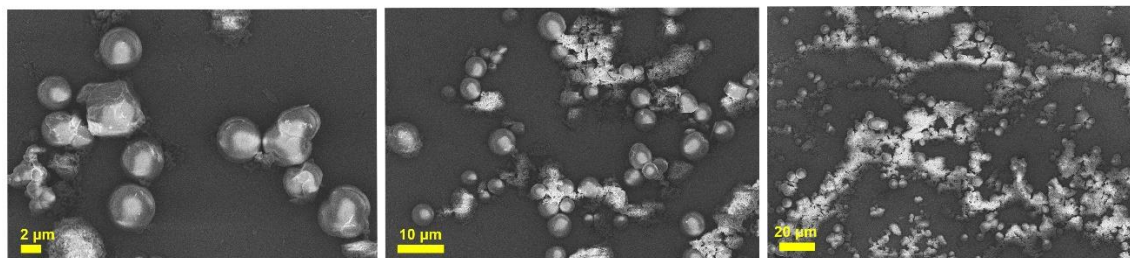


Fig. S3: Field Emission-Scanning Electron Microscopy (FESEM) images of **3** at different magnifications.

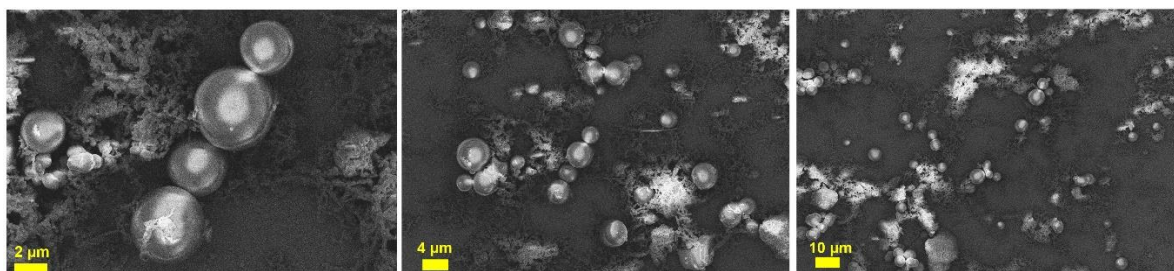
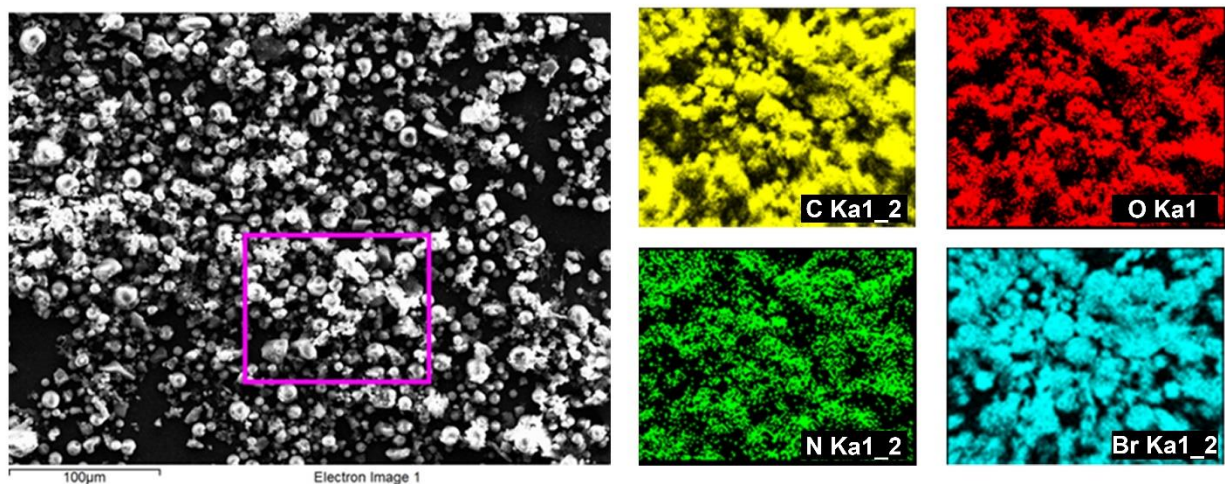


Fig. S4: FESEM images of **3_OH** at different magnifications.



IISERP-POF11 (1)

Element	Weight%	Atomic%
C K	68.13	76.87
N K	6.24	6.03
O K	18.81	15.94
Br L	6.82	1.16
Totals	100.00	

IISERP-POF12 (2)

Element	Weight%	Atomic%
C K	69.18	78.80
N K	5.47	5.34
O K	16.85	14.41
Br L	8.50	1.46
Totals	100.00	

IISERP-POF13 (3)

Element	Weight%	Atomic%
C K	64.71	77.69
N K	2.15	2.22
O K	19.58	17.65
Br L	13.56	2.45
Totals	100.00	

Fig. S5: FESEM-EDX elemental mapping of **1, 2 and 3**.

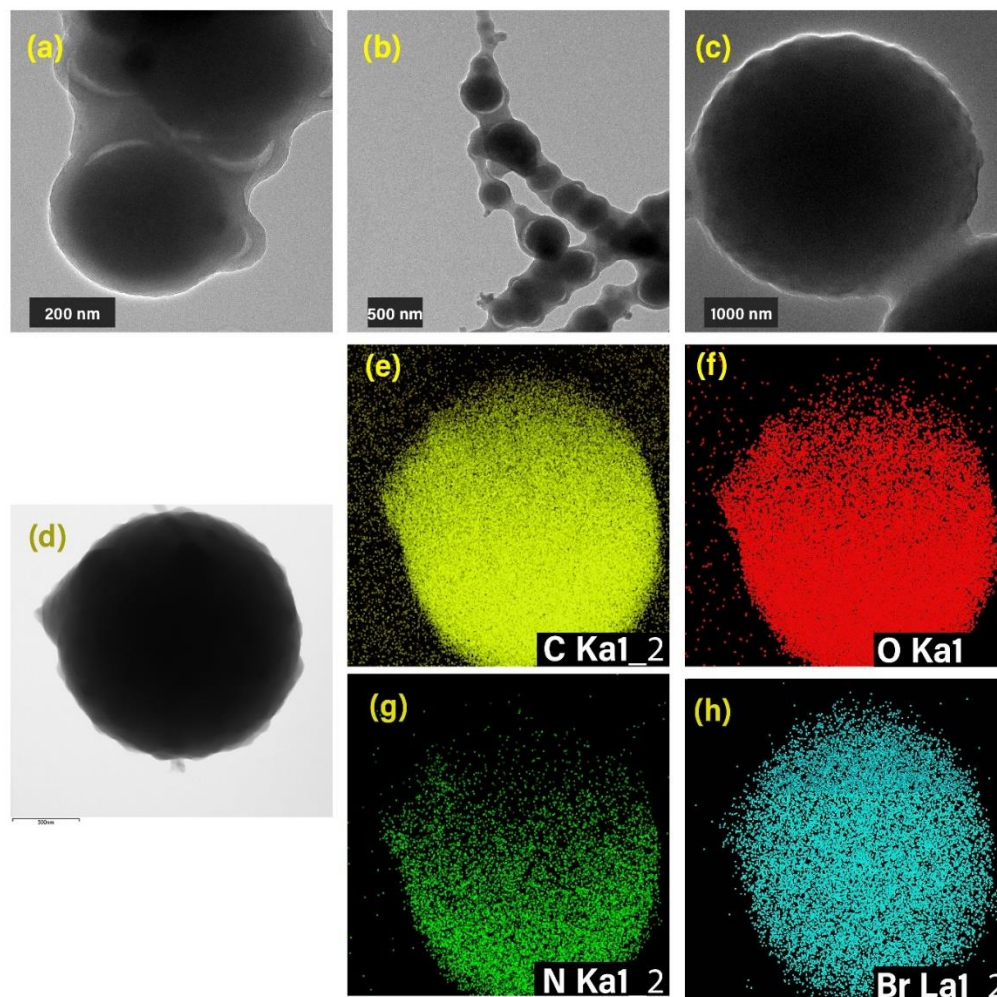


Fig. S6: High Resolution Transmission Electron Microscopy (HR-TEM) images of **2** at different magnifications.

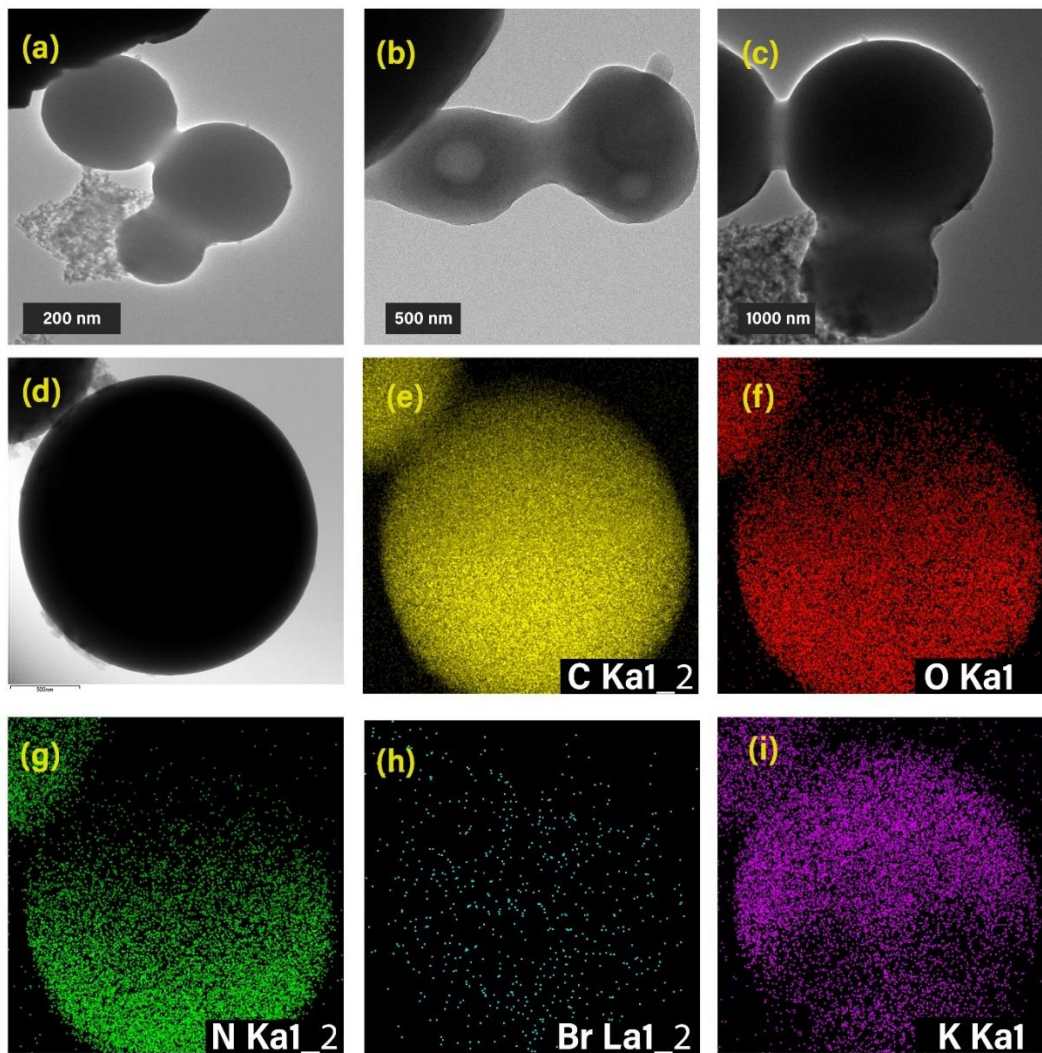


Fig. S7: HRTEM images of **2_OH** at different magnifications.

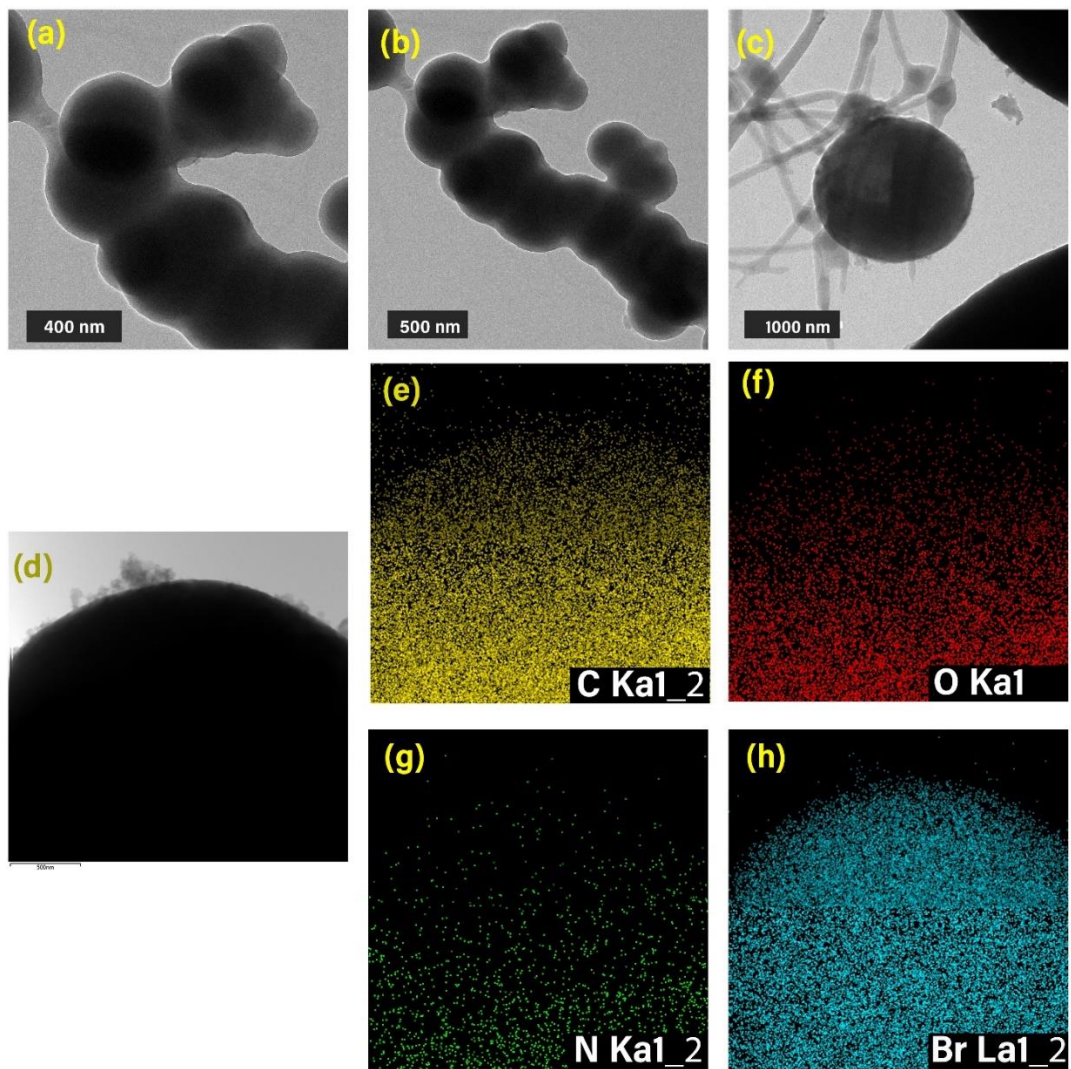


Fig. S8: High Resolution Transmission Electron Microscopy (HR-TEM) images of **3** at different magnifications.

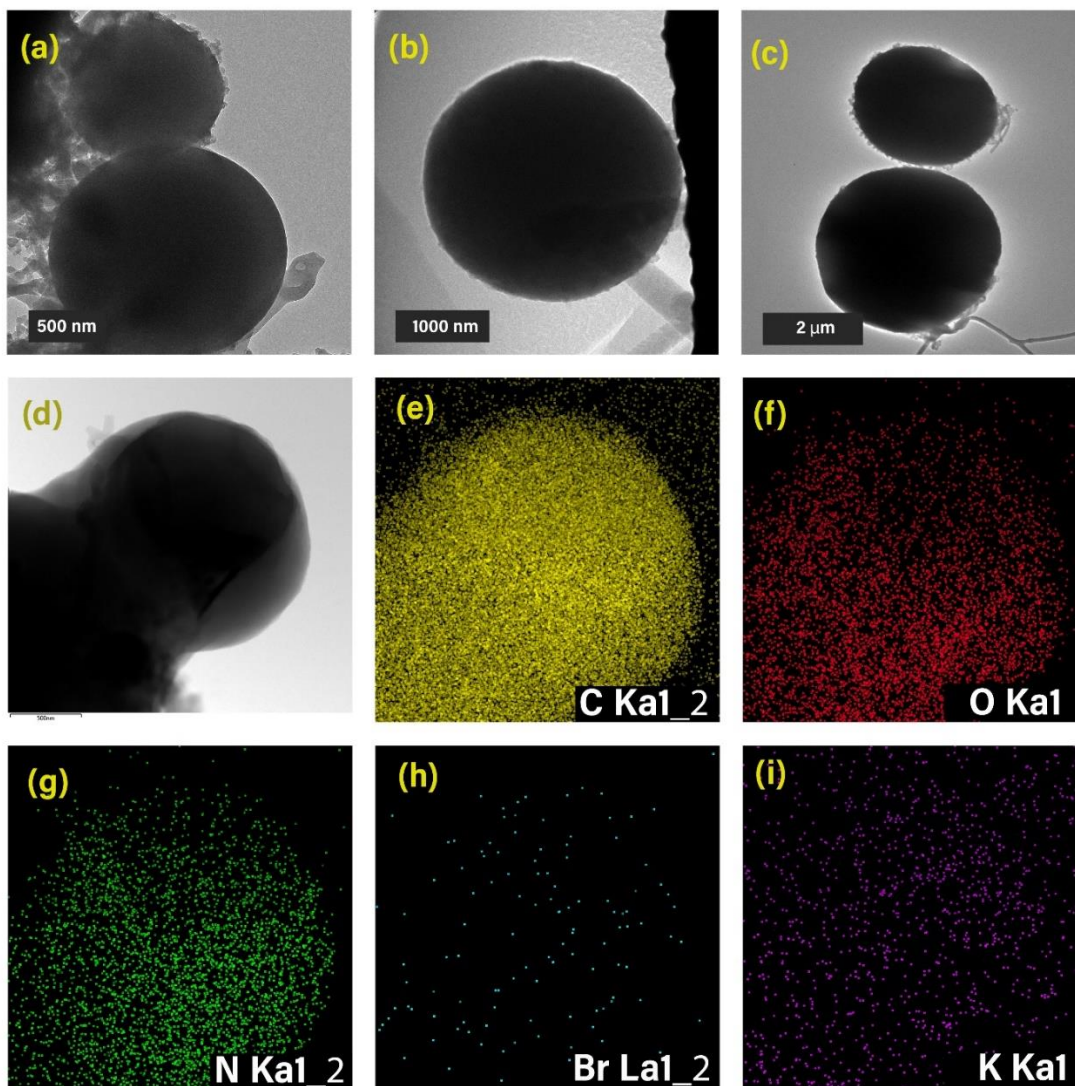


Fig. S9: HRTEM images of **3_OH** at different magnifications.

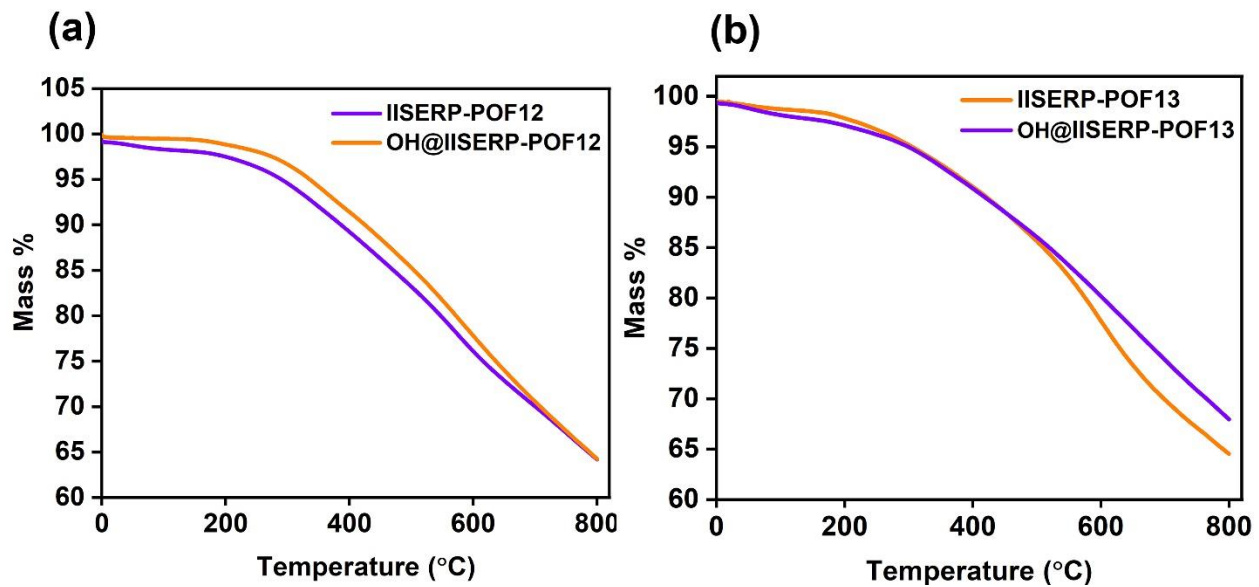


Fig. S10: (a) Comparative thermogravimetric analysis plot for 2, 2_OH and (b) 3, 3_OH.

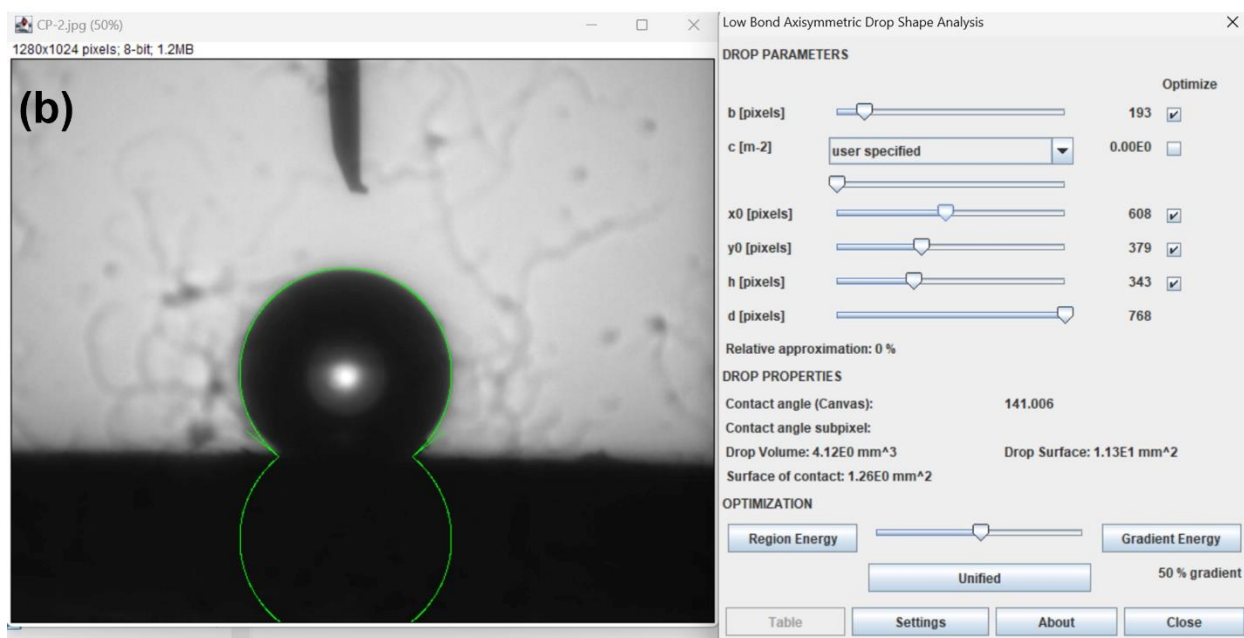
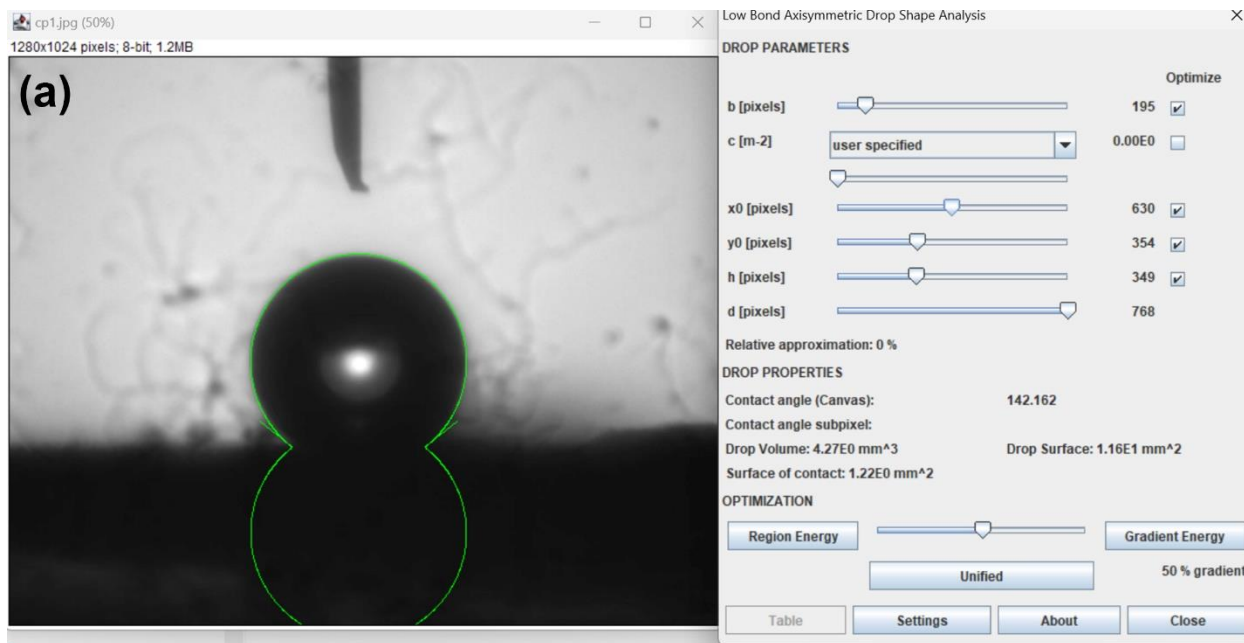


Fig. S11: (a) Contact angle of the droplet of water sitting on the surface of the (a) **2** and (b) **3**.

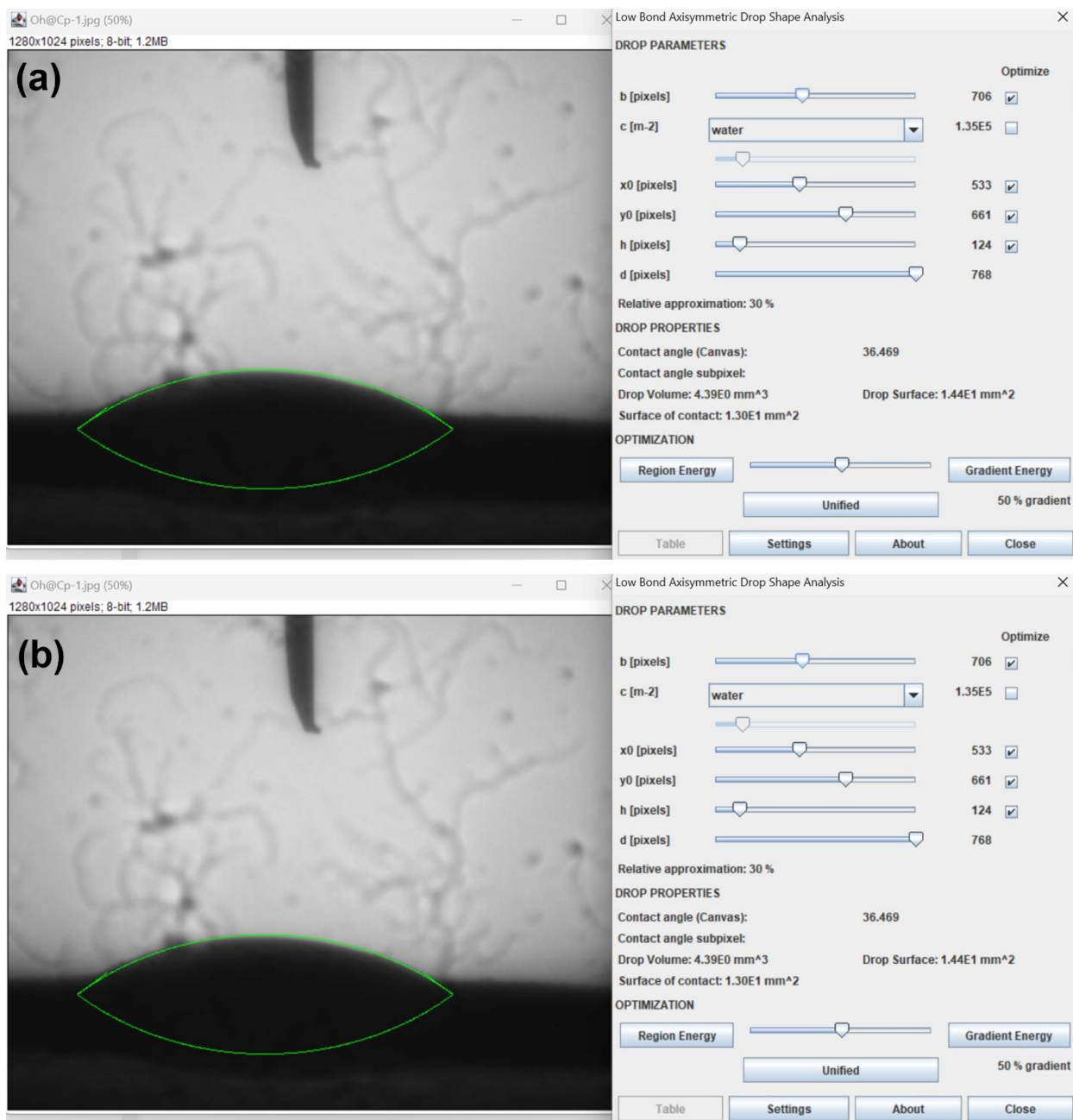


Fig. S12: Contact angle of the droplet of water sitting on the surface of the (a) **2_OH** and (b) **3_OH**.

Density Calculation

Density calculations were performed using an indirect method involving the mass and volume of the material. The volume calculation proceeded as follows: a fixed mass of the POF was filled in vials, marked, discharged, and then refilled with water up to the mark to determine the corresponding volume. It is acknowledged that the air trapped in the interparticle voids was not accounted for. To minimize this error, samples were meticulously prepared. All materials were thoroughly ground in a mortar and pestle before being sonicated to fine dispersive powders. After centrifugation, they were carefully filled into the vials to settle homogeneously. Each density calculation was performed three times to obtain a statistical average.

For the estimation of tap (bulk) densities, the samples underwent washing with methanol and acetone, followed by drying at 80 °C overnight to eliminate any solvent contributions. Subsequently, they were finely ground in a mortar and pestle to achieve a clump-free, free-flowing powder. A known weight of the powder was then transferred to the tap-density device, and the initial volume was recorded. The powder was subjected to 500 taps, and the final volume was recorded.

Note: The sample vial, post-tapping in a tilted position, demonstrates that the POF has settled tightly at the bottom without spilling out when tilted to 90 degrees.

Observation: Slight change in the tapped bulk densities of the samples 3 and 3_OH is observed.

Swelling study:

A pellet comprising 200 mg of POF sample was pressed, and parameters such as diameter and thickness were measured both in the dry state and under wet conditions. In the wet condition, the pellet was exposed to 95% relative humidity (RH) for 24 hours.

Observation: Minimal increase in both diameter and thickness is observed on exposing the 3 and 3_OH to 95 % RH for 24 hours.

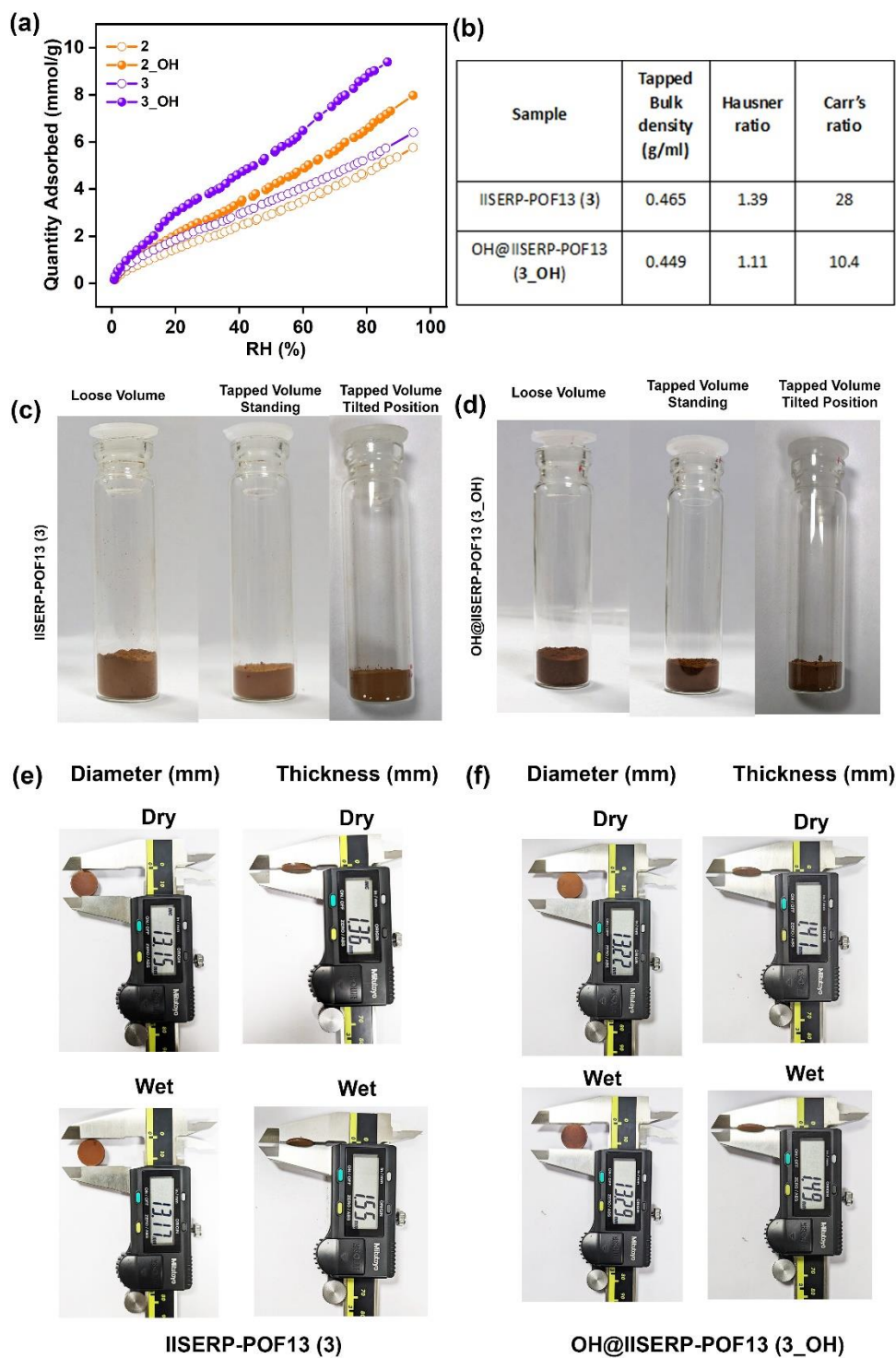


Fig. S13: (a) Comparative water adsorption isotherms of 2, 3, 2_OH and 3_OH (b) Density calculations using tapping method Photograph showing the volume change of (c) 3 and (d) 3_OH at different stages. Photograph showing the parameters of (e) 3 and (f) 3_OH before and after humidity exposure.

4. Hydroxide ion conductivity Analysis

4.1 Temperature-dependent hydroxide ion conductivity analysis of 2_OH and 3_OH :

The hydroxide ion conductivity (σ) of the 2, 3, 2_OH and 3_OH were investigated by the electrochemical impedance spectroscopy method from a frequency range of $1-10^6$ Hz using the Solartron Impedance Analyzer. For this, 2_OH and 3_OH were made into a pelletized form. The conductivity measurements were carried out three times on different pellet thicknesses (0.6 to 0.8 mm) and diameters of 10 mm to validate the consistency in the obtained results. Before each measurement, the sample was equilibrated at the particular temperature and humidity for 2 h throughout the experiment. The hydroxide ion conductivity of the pellet was measured from 25 to 80 °C in relative humidity (RH) of 95% and calculated using the following equation;

$$\sigma (\text{S cm}^{-1}) = \frac{l}{RA}$$

where l is the thickness of the pellet (cm), R is the resistance of the sample (Ω) obtained from the x-axis intercept, and A is the cross-sectional area of the pellet (cm^2). The humidity dependent OH^- ion conductivity of 2_OH and 3_OH were also measured at 80 °C with variable relative humidity under similar conditions.

4.2 Activation energy calculation for 2_OH and 3_OH

The activation energy was obtained using the Arrhenius equation where m is the slope of the plot between $\ln \sigma$ Vs $1000/T$ and the R is the gas constant with the value of 8.314 J/mol.

$$\ln \sigma = (-E_a/RT) + \ln A$$

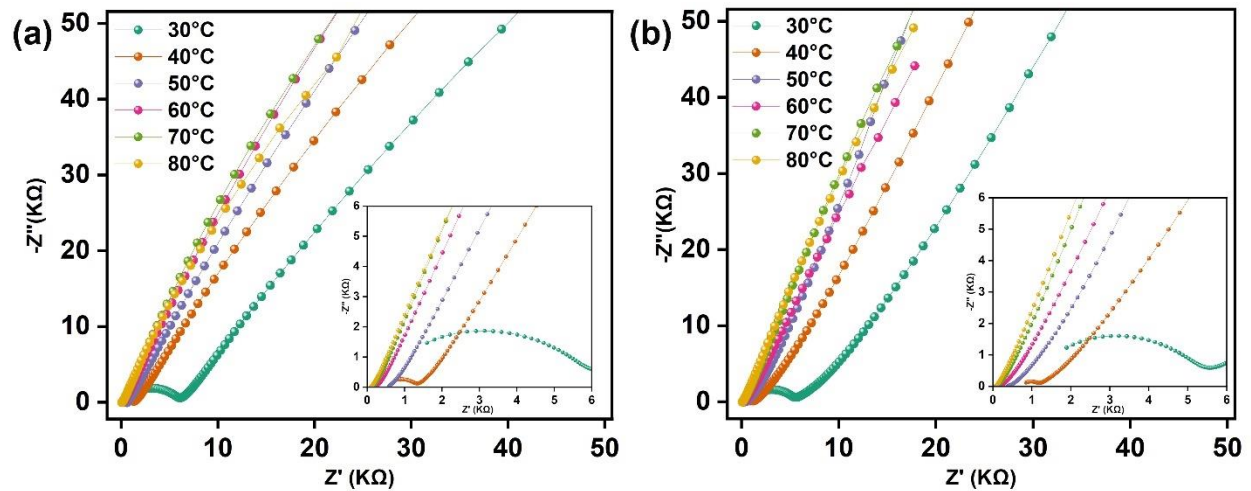


Fig. S14: Temperature dependent Nyquist plots of (a) 2, (b) 3 impedance analysis measured at 95 % RH .

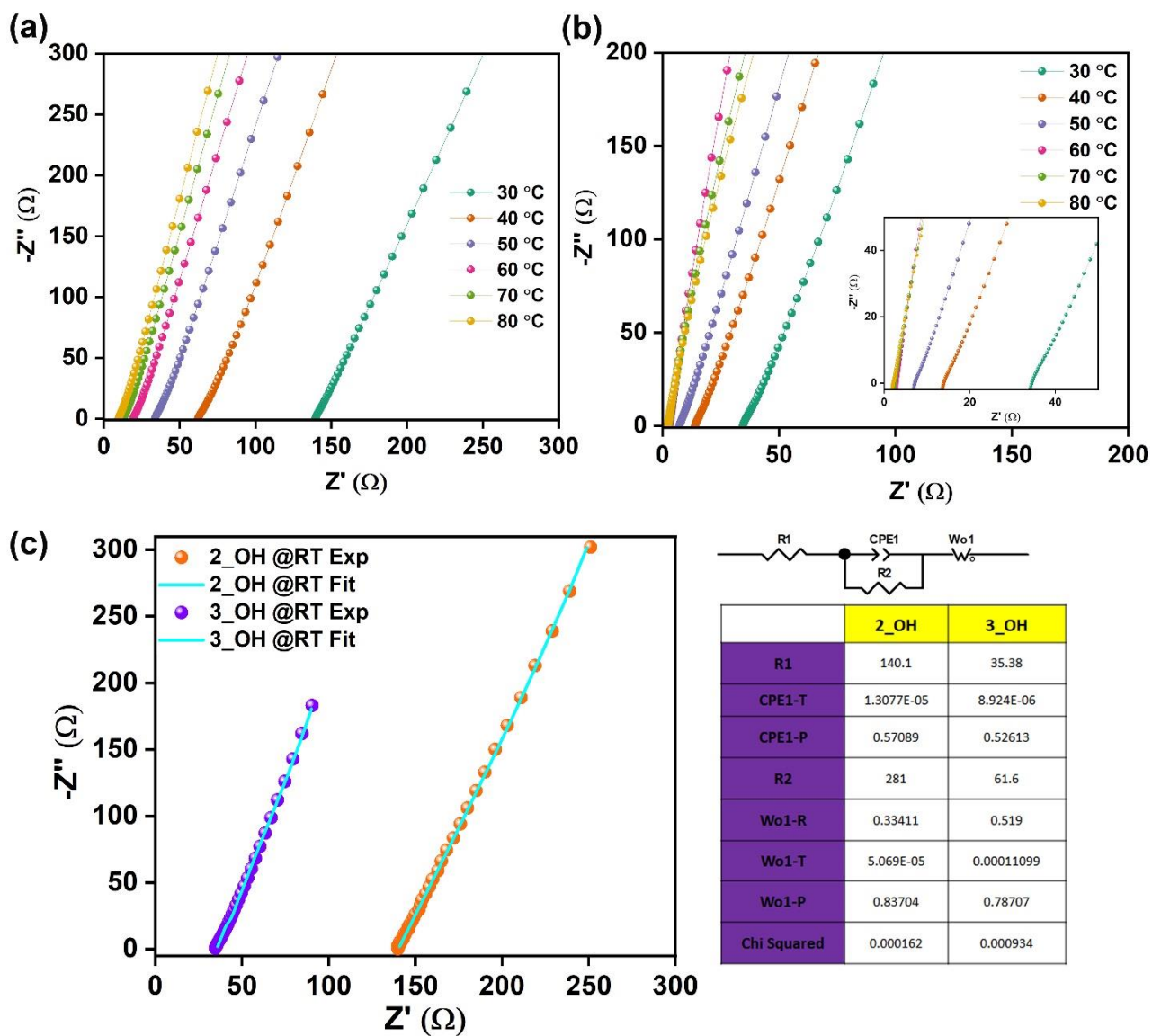


Fig. S15: Temperature dependent Nyquist plots of (a) 2_OH , (b) 3_OH impedance analysis measured at 95 % RH (c) Circuit fits for 2_OH and 3_OH impedance analysis measured at 80 °C and 95 % RH.

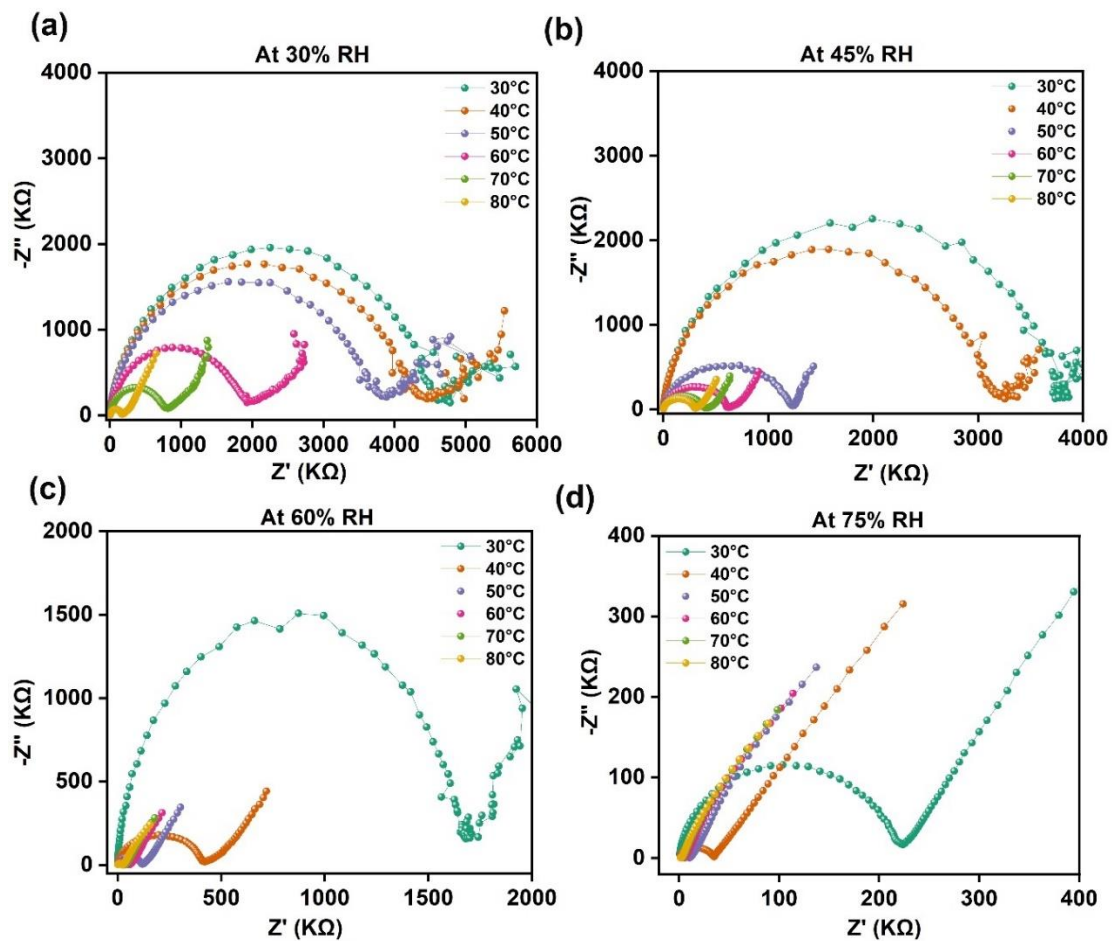


Fig. S16: Temperature dependent Nyquist plots of **2_OH** impedance analysis measured at (a) 30% (b) 45% (c) 60% (d) 75 % RH .

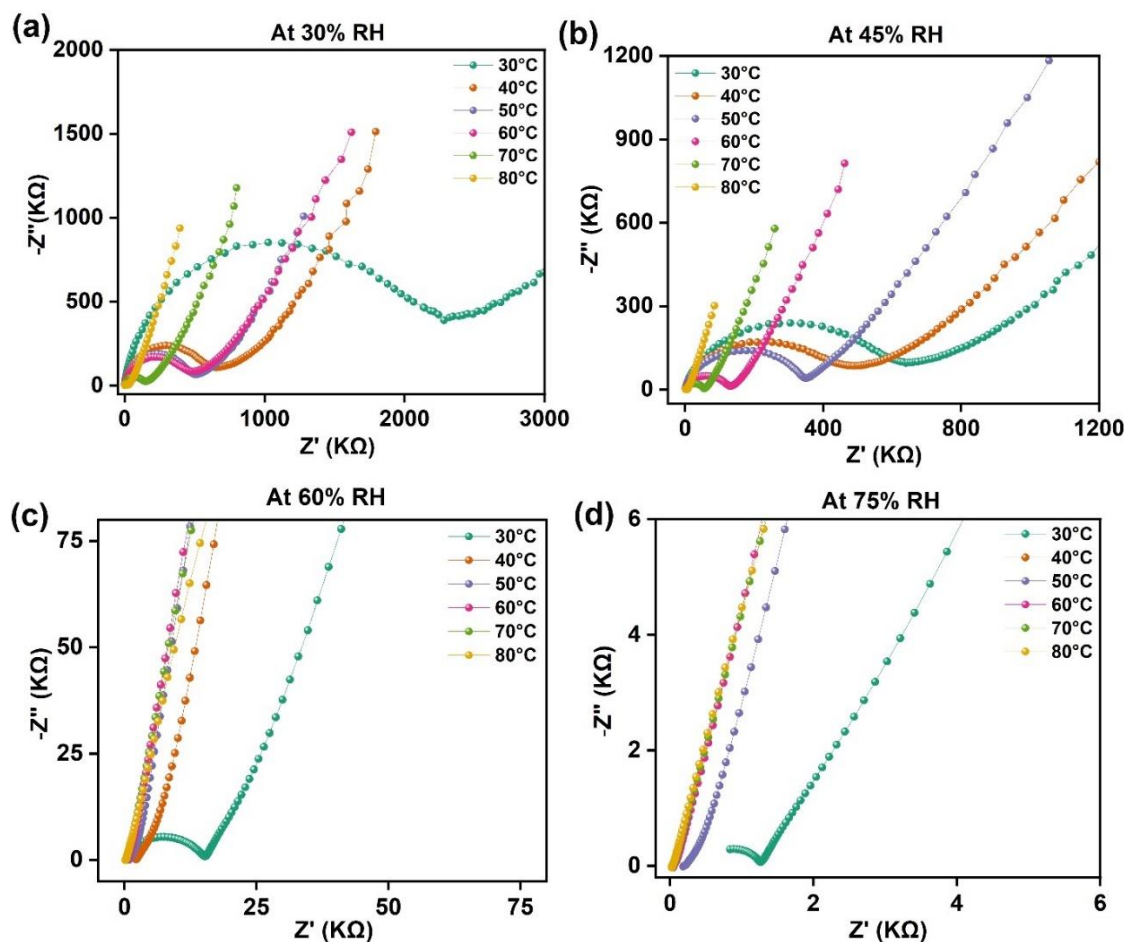


Fig. S17: Temperature dependent Nyquist plots of **3_OH** impedance analysis measured at (a) 30% (b) 45% (c) 60% (d) 75 % RH .

Table S1: Comparative hydroxide ion conductivity of **1_OH** at variable temperatures and a constant relative humidity of 95%.

Sr. No.	Relative Humidity (%)	Temperature (°C)	Conductivity γ (S/cm) 1_OH*	Conductivity (S/cm) 2_OH	Conductivity (S/cm) 3_OH
1	95	30	2.70E-04	7.30E-04	2.96E-03
2	95	40	1.40E-03	1.65E-03	9.45E-03
3	95	50	2.30E-03	3.03E-03	1.43E-02
4	95	60	3.40E-03	5.23E-03	2.00E-02
5	95	70	5.30E-03	7.89E-03	2.43E-02
6	95	80	1.40E-02	1.53E-02	4.88E-02

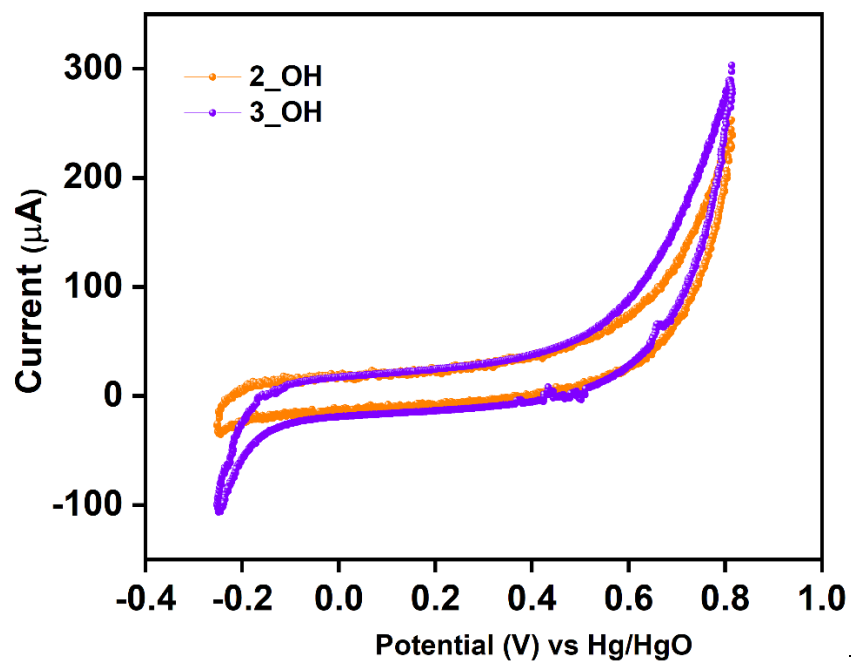


Fig. S18: Cyclic voltammogram of 2_OH and 3_OH measured using a three-electrode system in 1M KOH electrolyte with Hg/HgO as reference and Pt wire as counter electrode.

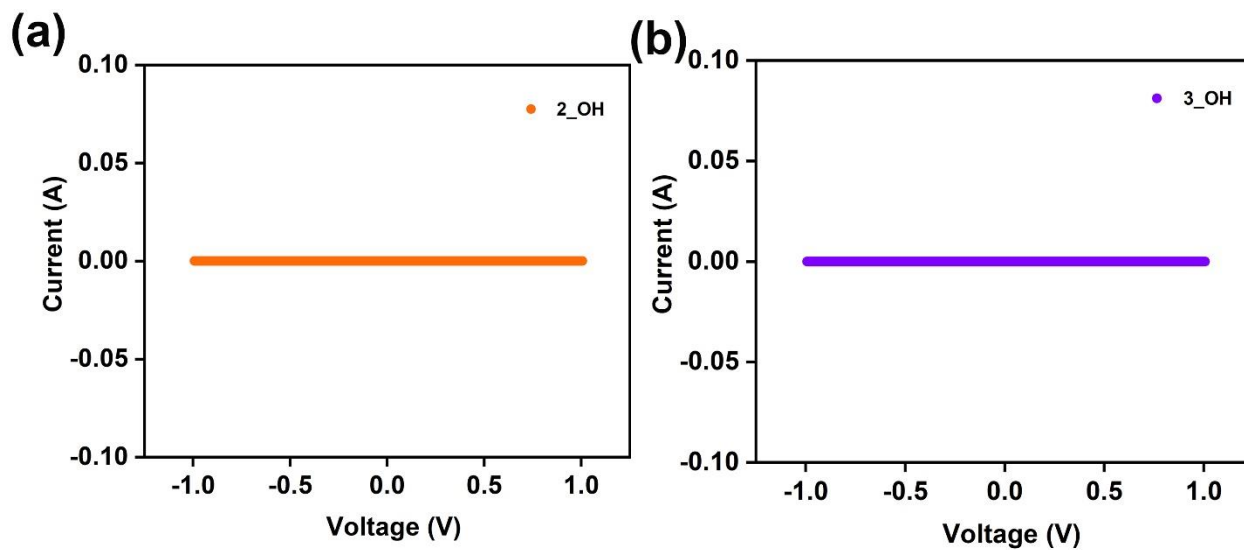


Fig. S19: I-V curve of 2_OH and 3_OH measured using a two-probe set-up.

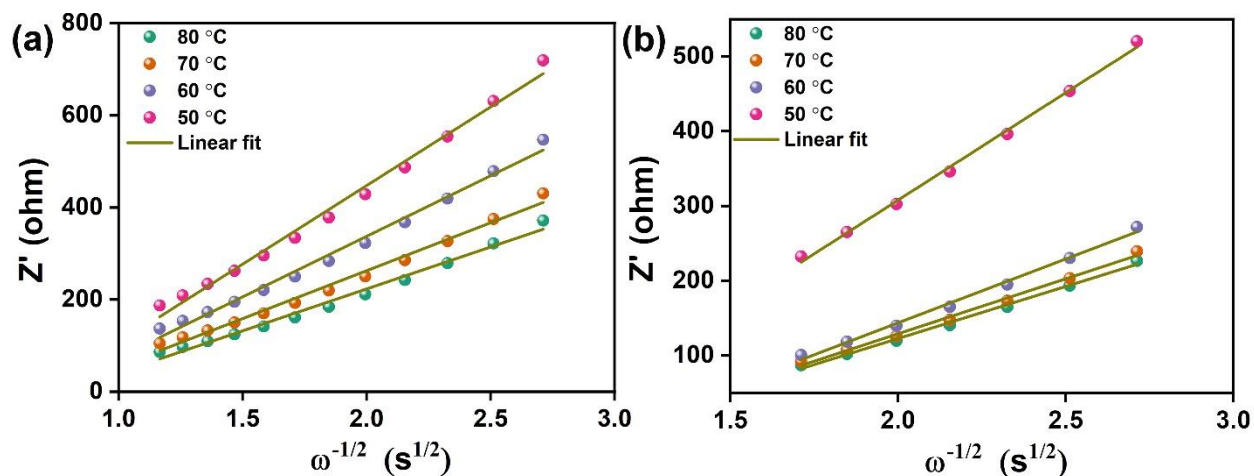


Fig. S20: A plot of the Z' versus $\omega^{-1/2}$ for (a) 2_OH and (b) 3_OH at 95% RH at different temperatures.

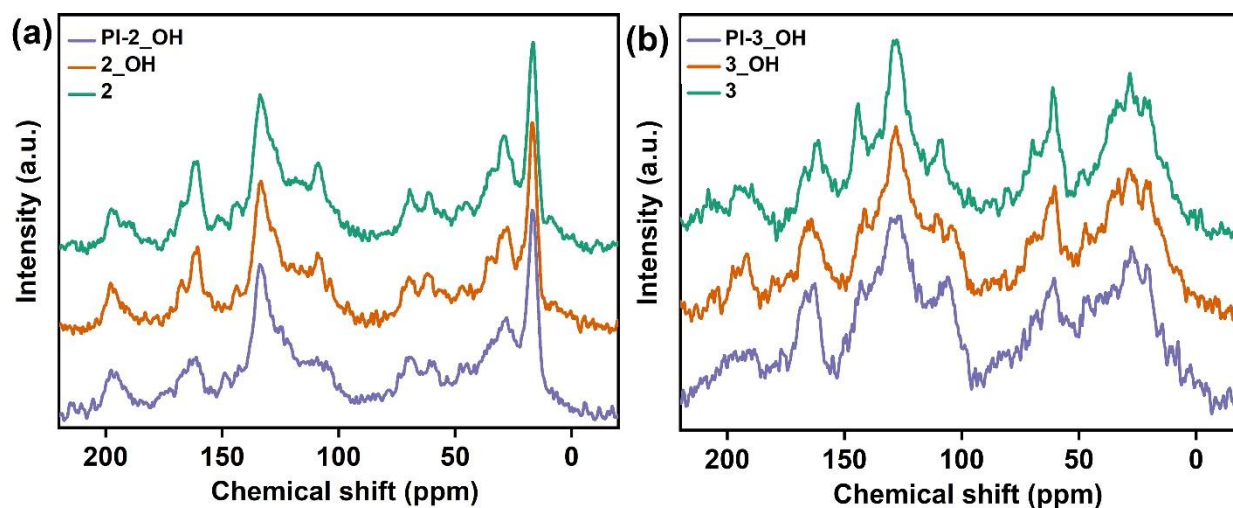


Fig. S21: Comparative Solid-state Cross-Polarization Magic Angle Spinning Carbon-13 Nuclear Magnetic Resonance (^{13}C CP-MAS NMR) spectra 2, 2_OH, PI-2_OH and 3, 3_OH, PI-3_OH.

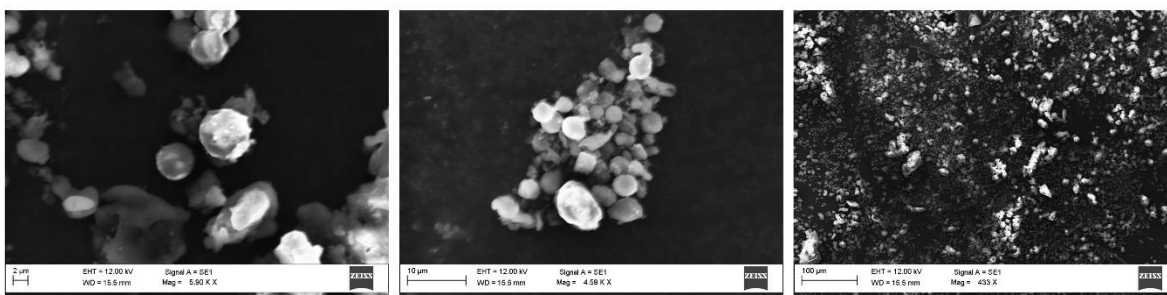


Fig. S22: Post impedance Field Emission-Scanning Electron Microscopy (FESEM) images of 2_OH at different magnifications.

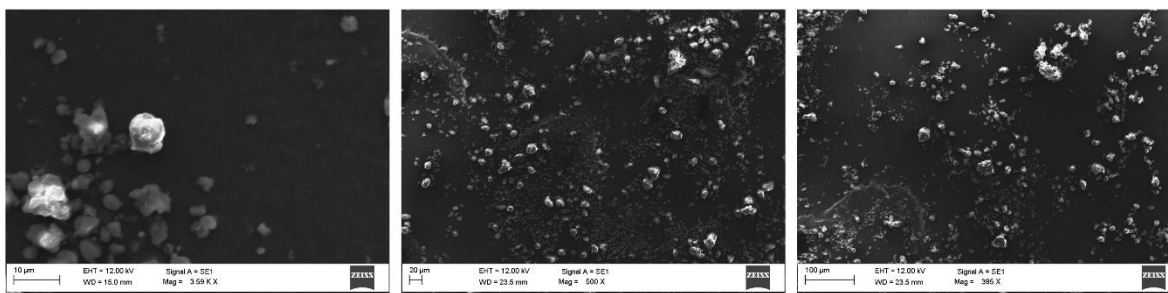


Fig. S23: Post impedance Field Emission-Scanning Electron Microscopy (FESEM) images of 3_OH at different magnifications.

5. Development of IISERP-POF13_OH@PVA (3_OH@PVA)

To prepare the mixture, 100 mg of 3_OH powder was dispersed in 2 ml of water and stirred at 90°C for 1 hour until a uniform distribution of the polymer was achieved. Subsequently, 100 mg of PVA was introduced into the same solution, and the mixture was heated for 3 hours to ensure a homogeneous blend of POF (3_OH) and PVA. As soon as the PVA had completely dissolved in the water, the solution was poured into a petri dish and promptly subjected to a cooling process. The cooling procedure involved two stages: initially at -20 °C for 3 hours, followed by a subsequent stage at 0 °C for 2 hours. After this cooling process, the resultant membrane solidified. The solidified membrane was then air-dried at room temperature, resulting in the formation of a flexible membrane. This flexible membrane was subsequently employed as a combined separator and electrolyte within the context of a Zinc air battery application.

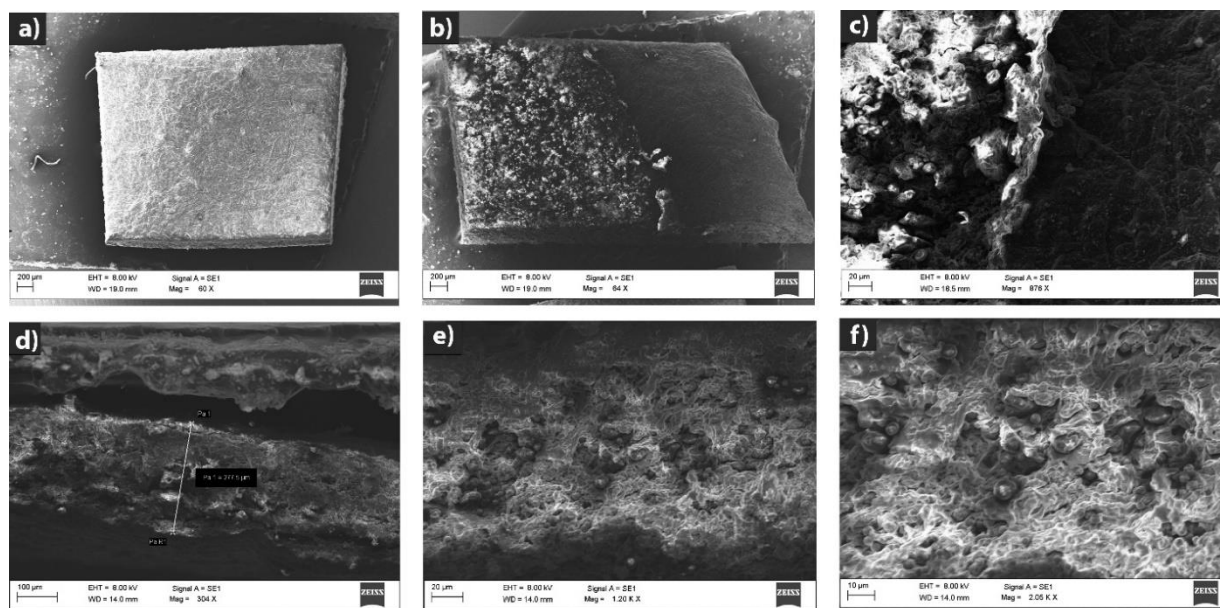


Fig. S24: FESEM images of 3_OH@PVA membrane at different magnifications.

Amplitude Roughness Parameters (Flatness Index)

Based on the provided AFM images and amplitude roughness parameters, it is evident that the flatness of the electrolyte membrane is well within the desired range. The Mean Surface Roughness (S_a) values, ranging from 177 nm to 268 nm across different samples, demonstrating that the membrane maintains a consistent level of flatness.

Examining the Root Mean Square Height of the surface (S_q), the values range from 223 nm to 350 nm, further corroborating the findings regarding surface roughness. Despite slight variations between samples, the S_q values remain within reasonable limits, confirming the uniformity of the membrane surface.

In conclusion, the analysis of the amplitude roughness parameters and AFM images indicates that the electrolyte membrane exhibits satisfactory flatness characteristics. The consistent S_a values, along with the S_q , S_{ku} , S_p , and S_z parameters, confirm the uniformity and stability of the membrane surface. These findings suggest that the membrane is well-suited for applications where flatness is crucial factor.

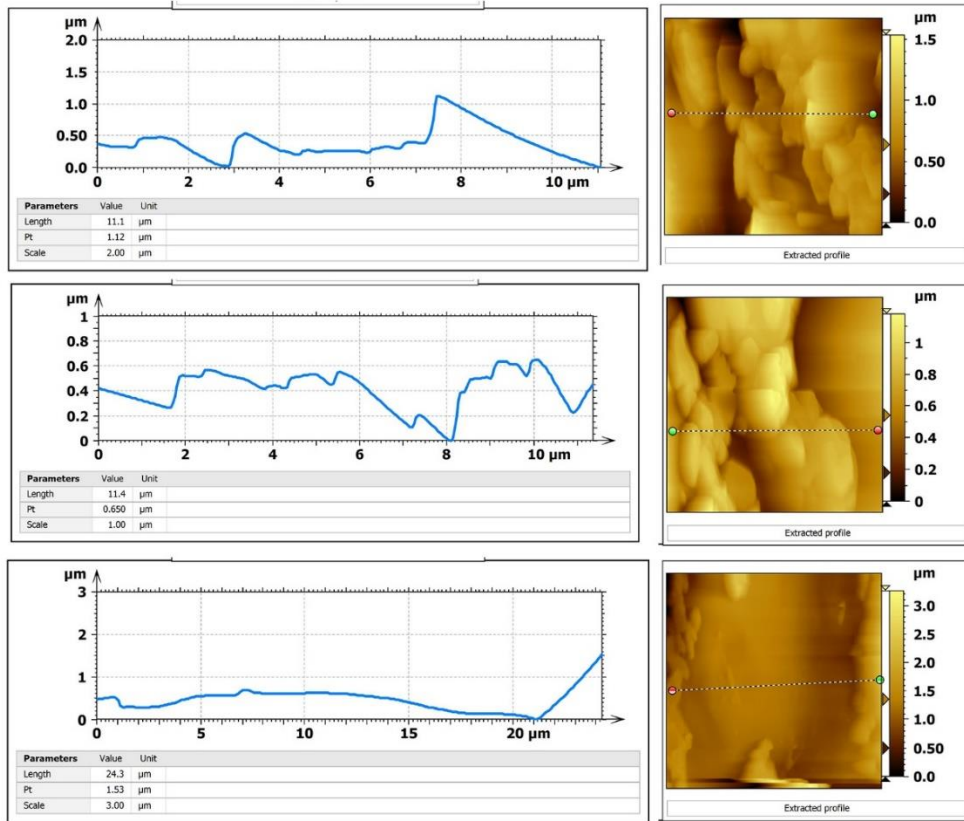


Fig S25: Atomic Force Microscopy (AFM) images of 3-OH@PVA membrane scanned at different sample area.


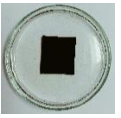

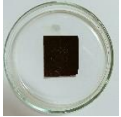
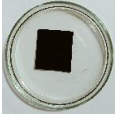

Table S2: Amplitude Roughness Parameters of different samples.

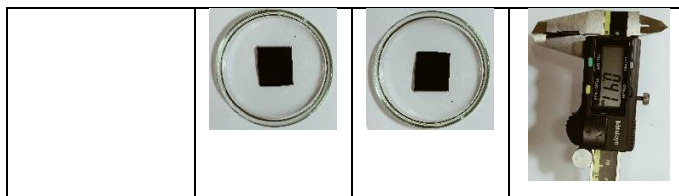
Amplitude Roughness Parameters	Sample-1	Sample-2	Sample-3
Sa (Mean Surface Roughness)	177 nm	167 nm	268 nm
Sq (Root mean square height of the surface)	223 nm	205 nm	350 nm
Sku (Kurtosis (fourth statistical moment, qualifying the flatness of the height distribution). Width of the height distribution.)	2.26	2.62	2.16
Sp (Height of highest peak)	903 nm	556 nm	990 nm
Sz (Defined as the average of the five highest local maximums plus the average of the five lowest local minimums.)	1.54 μm	1.19 μm	1.97 μm

Alkaline durability test

The durability test involved immersing the membrane in the solution for 12 hours, and the change in thickness was measured at each stage. Minimal change in membrane thickness was observed, indicating excellent alkali stability. No wear or tear was observed on the membrane throughout the test.

Table S3: The membrane thickness measurements before dipping, after dipping, and upon drying.

KOH Conc.	Membrane Thickness (mm)		
	Before Dipping	After Dipping	On Drying
2M	0.34 	0.38 	0.37 
4M	0.37 	0.39 	0.38 
6M	0.38	0.42	0.41



These results demonstrate the membrane's ability to maintain its integrity and thickness even after exposure to high concentrations of KOH solution for an extended period.

6. Battery studies

6.1. Fabrication of Zinc-Air Battery (ZAB):

The In-situ Analytical Split Test Cell for Lithium/Zinc-Air Battery setup was used to fabricate the Zinc-air battery where, zinc dust was used as the anode which was wetted with about 500 μL of 3 M KOH solution. The cathode was coated with Pt/C + RuO₂ (slurry in 1:1 EtOH: H₂O) on GDL (Gas Diffusion Layer). The amount of Pt/C + RuO₂ was maintained as 1 mg_{Pt}/cm² for the cathode. Finally, the cathode and anode were sandwiched with the prepared 3_**OH@PVA** as the separator-cum-electrolyte. The battery setup was assembled with screws and a continuous flow of O₂ gas was provided throughout the measurements. The polarization curves were obtained by performing the linear sweep voltammetry (LSV) from OCV to 0.4 V at a scan rate of 10 mV s⁻¹ using the AMETEK battery analyzer.

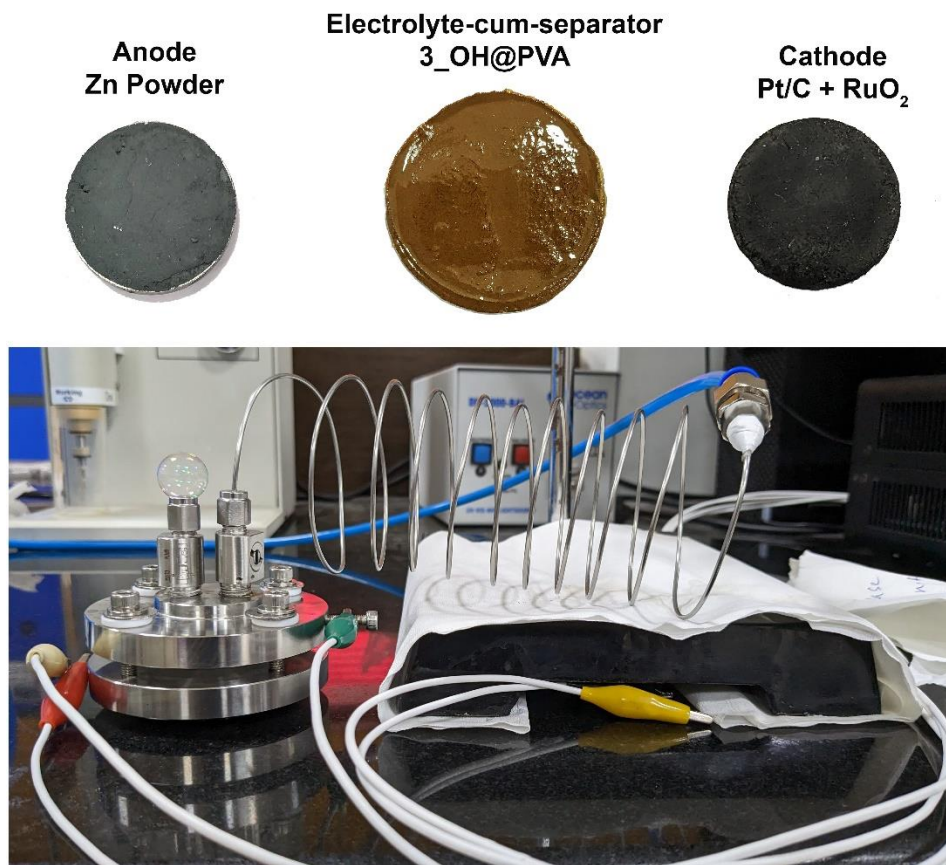


Fig. S26: Photographic images of the ZAB assembly. The process of creating, evaluating performance, and demonstrating the zinc-air battery (ZAB) involved the following steps: (a) A schematic illustration depicting the fabrication of the ZAB, where the cathode catalyst loading is set at 1.0 mg/cm², the anode employs zinc powder, and the separator consists of a 3_OH@PVA.

7. Post ZAB measurement sample characterizations

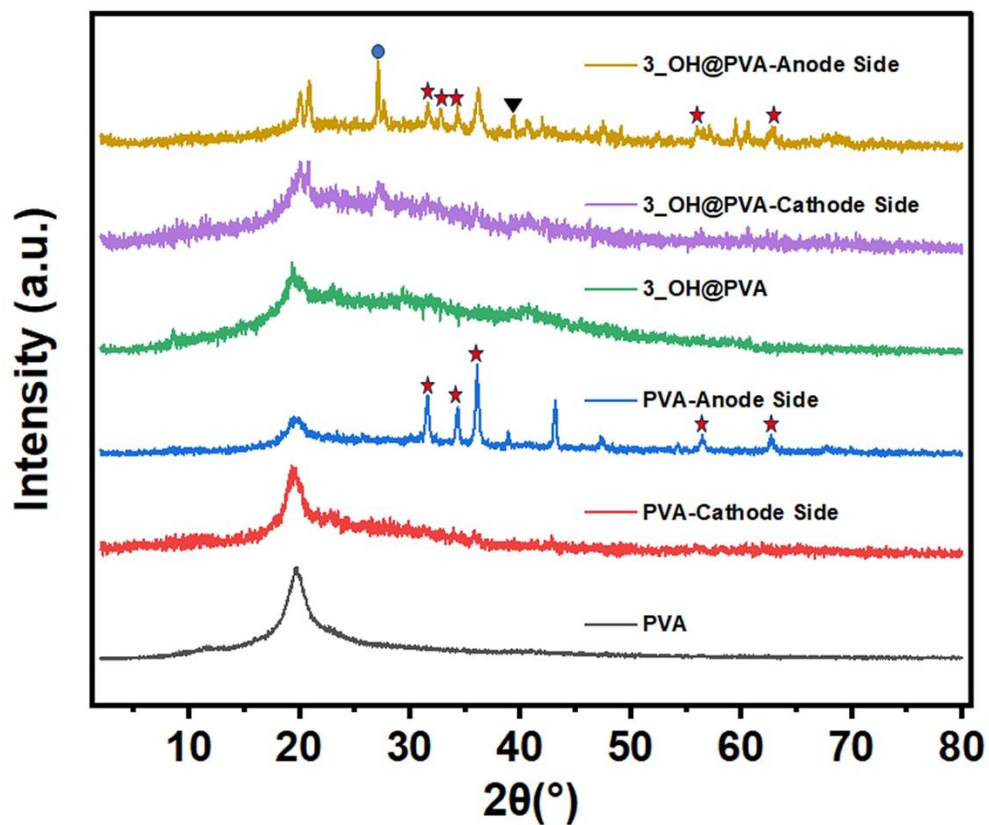


Fig. S27: Comparison of the PXRD patterns of the PVA, 3_OH@PVA. The inorganic species in this pyrolyzed sample includes ZnO(★), K_2CO_3 (●) and Pt_3O_4 (▼)(from cathode).

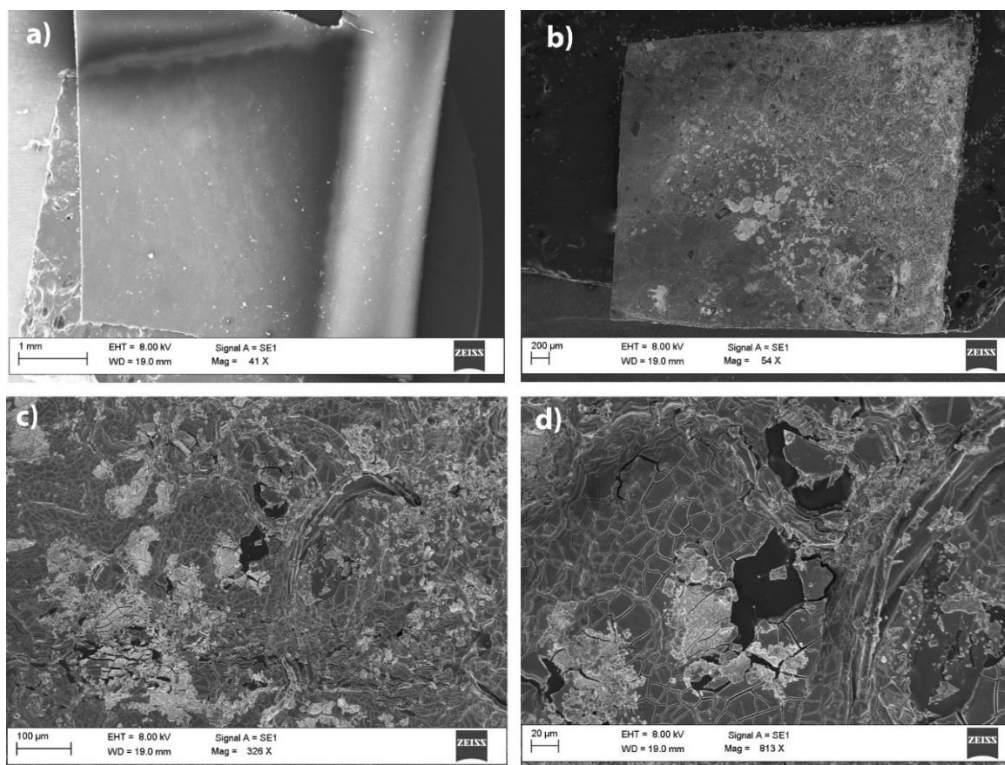


Fig. S28: FESEM images of PVA membrane (a) Pre battery measurements (b) Post battery measurements at different magnifications.

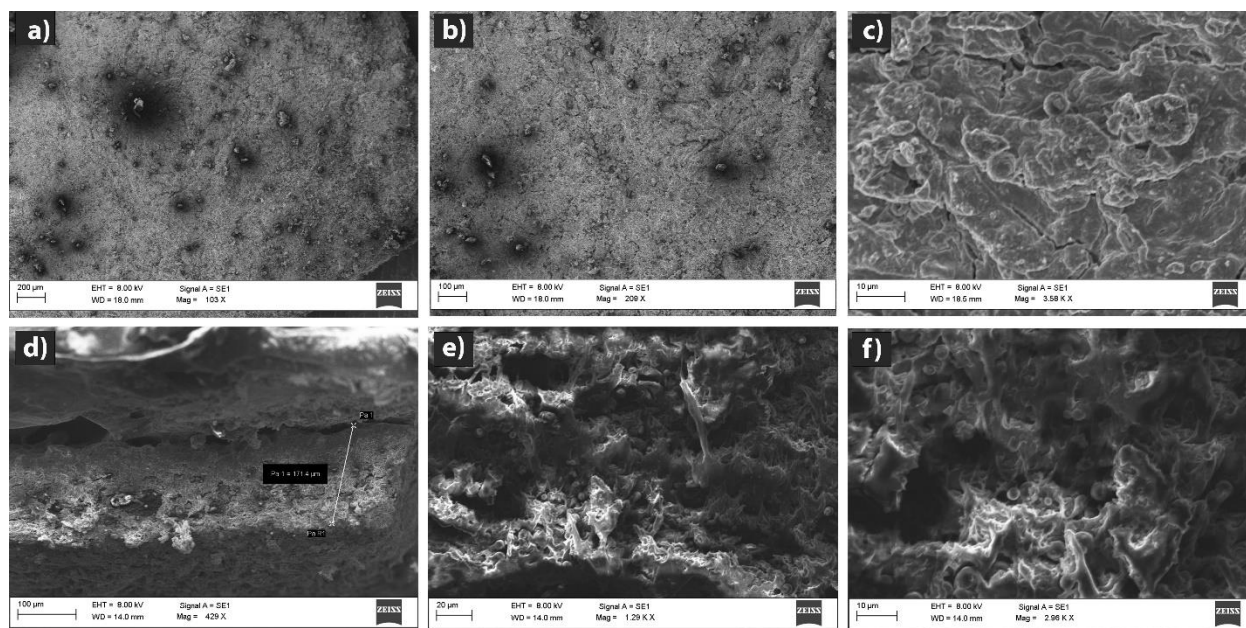


Fig. S29: The FESEM images of the post-battery measurement electrolyte (3_OH@PVA) showed lowering in thickness compared to the 3_OH@PVA pre battery measurements.

Table S4: Comparison of the RZAB of the **3_OH** with relevant literature reports.

Sr. No.	Bifunctional catalysts	Hydrogel/Solid-state electrolyte	Current density (mA cm ⁻²)	Power density (mW cm ⁻²)	Cycle life (h)	Reference
1	FeNi SAs/NC	PVA-KOH	1	52.12	45	Adv. Energy Mater.2021, 11, 2101242
2	Pt/C+RuO ₂	PVA-KOH	1	45.25	20	Adv. Energy Mater.2021, 11, 2101242
3	FeCo/Se-CNT	PVA-KOH-Zn(Ac) ₂	5	37.5	70	NanoLett.2021, 21, 2255–2264
4	CS-NFO@PNC	PVA-KOH-Zn(CH ₃ COO) ₂	5	=	40	Appl. Catal. B-environ 2022, 300, 120752
5	Fe,Mn/N-C	PVA-KOH	5	160.8	81	NATURE COMMUNICATIONS (2021) 12:1734 https://doi.org/10.1038/s41467-021-21919-5
6	Co/ZnCo ₂ O ₄ @NC-CNTs	PVA-KOH-Zn(Ac) ₂	5	151	20	Nano Energy Volume 82, April 2021, 105710
7	Fe ₁ Co ₁ -CNF	PVA-18M KOH-0.02M Zn(OAc) ₂	2	-	3.5	Nano Energy Volume 87, September 2021, 106147
8	FeP/Fe ₂ O ₃ @NPCA	PVA-KOH-Zn(Ac) ₂	5	35.5	8.3	Adv.Mater.2020, 32, 2002292
9	NiCo ₂ S ₄ @g - C ₃ N ₄ -CNT	PVA -10M KOH	3	-	14	Adv.Mater.2019, 31, 1808281
10	1nm CoO _x	PVA-4M KOH -0.2M Zn(Ac) ₂	6	300	10	Adv.Mater.2019, 31, 1807468
11	Pt/C+RuO ₂	PVA-4M KOH -0.2M Zn(Ac) ₂	6	225	10	Adv.Mater.2019, 31, 1807468
12	Co -NiO	PVA -KOH	2	50	6	Applied Catalysis B: Environmental 2019, 250, 71
13	Co ₃ O ₄ @CC	PVA -2M KOH	2	-	10	Adv. Energy Mater.2017, 7, 1700779
14	Co ₄ N/CNW/CC	PVA -9M KOH	0.5	-	15	Journal of the American Chemical Society 2016, 138, 10226
15	V ₂ O ₃ /MnS	PVA-KOH	2	72	18	Small2022, 18, 2104411
16	CoMn ₂ O ₄ /NCNFs	PVA-KOH-ZnO	1	39.3	5	J. Mater. Chem. A, 2019, 7, 24868–24876
17	Pt/C+RuO₂	3_OH@PVA	5	158	67	This work

7. References

[S1] R. E. Gawley, H. Mao, M. M. Haque, J. B. Thorne, J. S. Pharr, *J. Org. Chem.* **2007**, 72, 2187.

- [S2] S. Nandi, J. Rother, D. Chakraborty, R. Maity, U. Werner-Zwanziger, R. Vaidhyanathan, *J. Mater. Chem. A* **2017**, *5*, 8431.
- [S3] D. Chakraborty, S. Nandi, R. Kushwaha, D. Kaleeswaran, R. Vaidhyanathan, *Mater. Res. Bull.* **2021**, 111614.